US Army Corps of Engineers

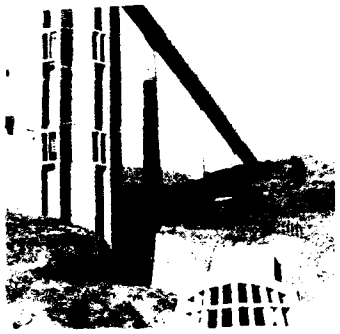

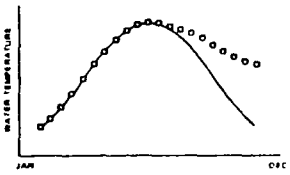

a. Real-daily operations

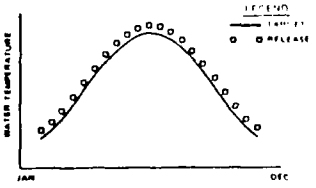

HYDRAULICS LABORATORY

TECHNICAL REPORT HL-89-13

(2)

INTAKE STRUCTURE OPERATION STUDY LOST CREEK DAM, OREGON

by

Stacy E. Howington

Hydraulics Laboratory

DEPARTMENT OF THE ARMY
Waterways Experiment Station, Corps of Engineers
PO Box 631, Vicksburg, Mississippi 39181-0631

July 1989
Final Report

Approved For Public Release; Distribution Unlimited

Prepared for US Army Engineer District, Portland
Portland, Oregon 97208-2946

SECURITY CLASSIFICATION OF THIS PAGE

REPORT DOCUMENTATION PAGE

Form Approved OMB No. 0704-0188

1a REPORT SECURITY CLASSIFICATION: Unclassified	1b RESTRICTIVE MARKINGS
2a SECURITY CLASSIFICATION AUTHORITY	3 DISTRIBUTION / AVAILABILITY OF REPORT: Approved for public release; distribution unlimited.
2b DECLASSIFICATION / DOWNGRADING SCHEDULE	
4 PERFORMING ORGANIZATION REPORT NUMBER(S): Technical Report HL-89-13	5 MONITORING ORGANIZATION REPORT NUMBER(S)
6a NAME OF PERFORMING ORGANIZATION: USAEWES Hydraulics Laboratory; 6b OFFICE SYMBOL (If applicable): CEWES-HS-H	7a NAME OF MONITORING ORGANIZATION
6c ADDRESS (City, State, and ZIP Code): PO Box 631 Vicksburg, MS 39181-0631	7b ADDRESS (City, State, and ZIP Code)
8a NAME OF FUNDING / SPONSORING ORGANIZATION: USAED, Portland; 8b OFFICE SYMBOL (If applicable)	9 PROCUREMENT INSTRUMENT IDENTIFICATION NUMBER
8c ADDRESS (City, State, and ZIP Code): PO Box 2946 Portland, OR 97208-2946	10 SOURCE OF FUNDING NUMBERS: PROGRAM ELEMENT NO. / PROJECT NO. / TASK NO. / WORK UNIT ACCESSION NO.

11 TITLE (Include Security Classification)

Intake Structure Operation Study, Lost Creek Dam, Oregon

12 PERSONAL AUTHOR(S)
Howington, Stacy E.

13a TYPE OF REPORT	13b TIME COVERED	14 DATE OF REPORT (Year, Month, Day)	15 PAGE COUNT
Final report	FROM _____ TO _____	July 1989	82

16 SUPPLEMENTARY NOTATION
Available from National Technical Information Service, 5285 Port Royal Road, Springfield, VA 22161.

17 COSATI CODES		
FIELD	GROUP	SUB-GROUP

18 SUBJECT TERMS (Continue on reverse if necessary and identify by block number)
Numerical modeling; Reservoirs; OSPACE (computer program); Resource conservation; Reservoir modeling; Water quality

19 ABSTRACT (Continue on reverse if necessary and identify by block number)

This report documents an investigation into reservoir release operations at the Lost Creek Dam, Oregon. The dam is located on the pristine Rogue River which provides habitat to a valuable anadromous fishery. This fishery is highly temperature sensitive. The US Army Engineer District, Portland, presently uses multiple-level selective withdrawal technology to meet the established downstream temperature targets that would best suit the fishery. These target temperatures are being adequately approximated in the releases for portions of the year. However, in the fall, winter, and early spring, the releases are warmer than desired. This problem is thought to be contributing to a lower-than-desirable survival rate among the young salmonids. The study documented herein provided a means of predicting the intake port openings to meet the desired release temperature most closely and investigated the potential for improving the long-term operational strategies for this structure.

(Continued)

20 DISTRIBUTION / AVAILABILITY OF ABSTRACT	21 ABSTRACT SECURITY CLASSIFICATION
☒ UNCLASSIFIED/UNLIMITED ☐ SAME AS RPT ☐ DTIC USERS	Unclassified
22a NAME OF RESPONSIBLE INDIVIDUAL	22b TELEPHONE (Include Area Code) / 22c OFFICE SYMBOL

DD Form 1473, JUN 86 *Previous editions are obsolete.* SECURITY CLASSIFICATION OF THIS PAGE

19. ABSTRACT (Continued).

To develop a prediction capability for the intake structure, the site-specific characteristics of selective withdrawal and simultaneous multiple-level withdrawal were studied. A 1:80-scale physical model was constructed and tested in both density-stratified and homogeneous density environments. The results of these studies were incorporated into an existing numerical model (SELECT) that predicts intake port openings to achieve release targets. The results of the physical model work followed logically that from similar, previously conducted studies.

The OSPACE model, an optimization routine surrounding a one-dimensional reservoir thermal model, was then used to evaluate the effects of short-term operational modifications on the reservoir's long-term ability to meet release targets. Each day in the year was assigned a priority and a release temperature deviation tolerance by the sponsor. These data were used to develop a function for comparing the relative worth of meeting prescribed targets during different periods. These evaluations indicated that some potential for improving the fall release temperatures existed, but only by sacrificing the agreement between releases and targets during the summer. An alternative set of target temperatures was produced that provide inherent resource conservation when used on a daily basis in lieu of the original targets.

Appendix A gives the withdrawal angle test results from the selective withdrawal evaluation. Appendix B shows the computation of the reliability index used during model verification.

PREFACE

This report was sponsored by the US Army Engineer District, Portland (NPP), as part of a combined physical/numerical model study of intake structure operations at the Lost Creek Dam, Oregon.

The study was conducted by personnel of the Hydraulics Laboratory (HL), US Army Engineer Waterways Experiment Station (WES), during the period September 1984 to December 1987. The study was conducted under the direction of Messrs. H. B. Simmons, former Chief, HL; F. A. Herrmann, Jr., Chief, HL; J. L. Grace, Jr., former Chief of the Hydraulic Structures Division (HSD); and G. A. Pickering, Chief, HSD. The tests were conducted by Mr. Stacy E. Howington, Reservoir Water Quality Branch (RWQB), HSD, under the direct supervision of Dr. J. P. Holland, Chief, RWQB, and Dr. R. E. Price, former Acting Chief, RWQB. This report was prepared by Mr. Howington, and edited by Mrs. Marsha C. Gay, Information Technology Laboratory, WES.

COL Dwayne G. Lee, EN, was the Commander and Director of WES. Dr. Robert W. Whalin was Technical Director.

This report should be cited as follows:

Howington, Stacy E. 1989 (Jul). "Intake Structure Operation Study, Lost Creek Dam, Oregon," Technical Report HL-89-13, US Army Engineer Waterways Experiment Station, Vicksburg, MS.

CONTENTS

	Page
PREFACE	1
CONVERSION FACTORS, NON-SI TO SI (METRIC) UNITS OF MEASUREMENT	3
PART I: INTRODUCTION	4
Background	4
The Problem	8
PART II: SELECTIVE WITHDRAWAL	11
Background	11
Intake Structure Physical Model	15
Selective Withdrawal Test Results	21
PART III: SIMULTANEOUS MULTILEVEL WITHDRAWAL	27
Concurrently Developed Theory	27
Algorithm Modifications for Lost Creek Application	28
Physical Model Work	30
PART IV: LONG-TERM OPERATIONAL STRATEGY OPTIMIZATION	40
OSPACE Background	40
WESTEX Verification and Final Verification	44
Application of OSPACE to Lost Creek	48
Model-Suggested Target Temperature Modifications	65
PART V: RESULTS AND CONCLUSIONS	70
REFERENCES	73
APPENDIX A: WITHDRAWAL ANGLE TEST RESULTS	A1
APPENDIX B: COMPUTATION OF THE RELIABILITY INDEX	B1

CONVERSION FACTORS, NON-SI TO SI (METRIC) UNITS OF MEASUREMENT

Non-SI units of measurement used in this report can be converted to SI (metric) units as follows:

Multiply	By	To Obtain
acres	4046.856	square metres
acre-feet	1,233.489	cubic metres
cubic feet	0.02831685	cubic metres
degrees (angle)	0.01745329	radians
feet	0.3048	metres
gallons	3.785412	cubic decimetres
inches	25.4	millimetres
miles (US statute)	1.609344	kilometres
pounds (mass) per cubic foot	16.01846	kilograms per cubic metre
square miles	2.589998	square kilometres

INTAKE STRUCTURE OPERATION STUDY, LOST CREEK DAM, OREGON

PART I: INTRODUCTION

Background

1. Lost Creek Lake is located 158 river miles from the Pacific Ocean on the main stem of the Rogue River in southwestern Oregon. Situated in the northeastern portion of the Rogue River Basin on the western slope of the Cascade Mountain Range (Figure 1), the dam is maintained and operated by the US Army Engineer District (USAED), Portland.

2. The lake is classified as dendritic. At a maximum pool elevation of 1,872,* it has an approximate surface area of 3,431 acres,** a volume of 465,000 acre-feet, and a length of about 10 miles. The maximum depth of the

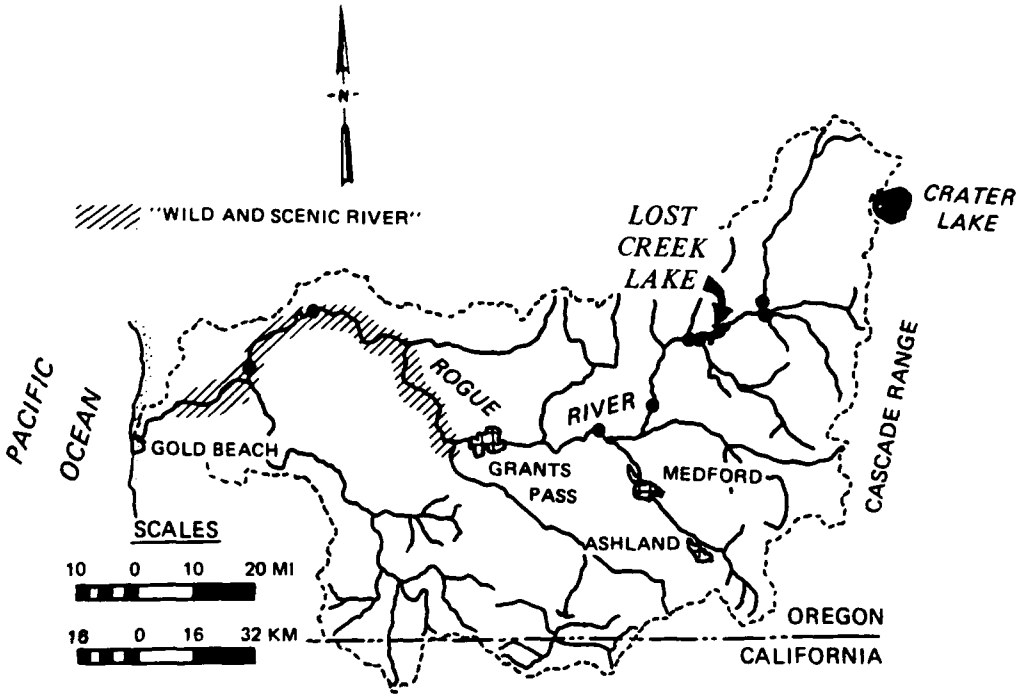

Figure 1. Location of Lost Creek Lake

---

* All elevations (el) and stages cited herein are in feet referred to the National Geodetic Vertical Datum (NGVD).

** A table of factors for converting non-SI units of measurement to SI (metric) units is found on page 3.

reservoir is about 322 ft, also measured at maximum pool elevation. Minimum conservation pool is at el 1,751.

3. There are two primary inflows to Lost Creek Lake. The Rogue River provides a majority of the inflow with the South Fork providing most of the remainder. Preimpoundment flow measurements in the Rogue River near the present lake site indicate an average inflow of 1,800 cfs. The average retention time is about 126 days (Cassidy, Larson, and Putney 1981).

4. The Lost Creek Lake watershed is mountainous and timber covered. It is usually subjected to mild, wet winters and warm, dry summers produced by the maritime and coastal mountain range influences. The drainage area of the reservoir is 674 square miles. Average annual rainfall at the reservoir is about 40 in. while at the headwaters, it is about 80 in. (USAED, Portland, 1966).

5. Construction of the Lost Creek Dam began in June 1972 and was completed in 1976 with impoundment beginning early in 1977. The authorized project purposes of Lost Creek Dam, as part of the Rogue River Basin Project, are flood control, irrigation, water supply, power generation, fish and wildlife enhancement, recreation, and water quality (Cassidy and Johnson 1982).

6. Releases from the reservoir are made almost exclusively through the unique, 257-ft-tall intake structure. This concrete structure is located in the hillside that constitutes the right abutment facing downstream. Only during extreme flood events is the need to use the overflow spillway (located near the left abutment) anticipated. The intake structure is composed of 12 individually operable intake ports, which all lead to a single, 30-ft-diam cylindrical wet well. The intake ports are configured in four sets of three ports each. All three ports within each set are at the same elevation, are evenly spaced, and are at 55-deg offsets incrementally in plan view. The four invert elevations of the port sets are 1,845, 1,790, 1,730, and 1,640.

7. During construction of the intake structure, the center port of the triad at el 1,640 was retrofitted with what is being termed an elephant trunk for release of potentially turbid waters from the bottom of the reservoir. This is actually a long, rectangular-exterior, circular-interior, concrete conduit also used for temperature control of the release water. The trunk extends downward to an invert elevation of 1,595. This addition resulted in five intake elevations with three intakes at each of the top three levels, two at the fourth level, and one at the fifth as seen in Figure 2. Some of the

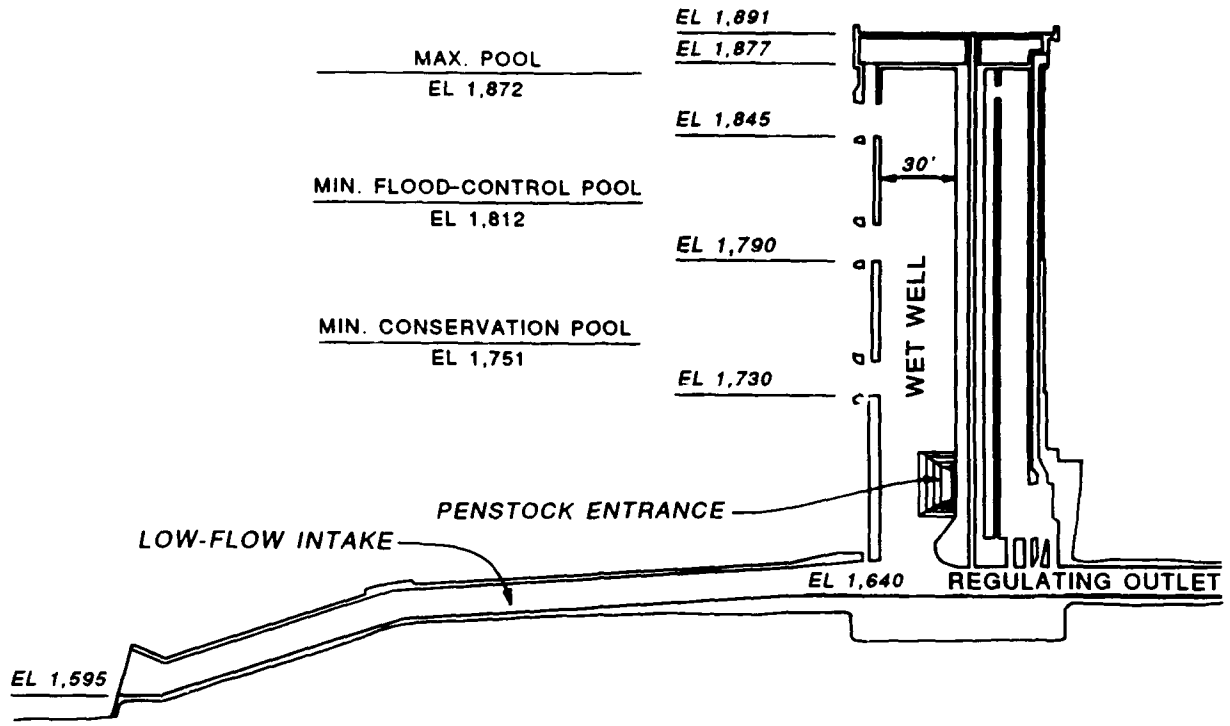

Figure 2. Schematic of the Lost Creek Lake intake structure (after USAED, Portland, 1983)

intakes, including the elephant trunk, can be seen in Figure 3.

8. Each of the top 11 intake ports is 8 ft wide and 15 ft tall with an individually operable slide gate. The edges of the entrances to the intakes are well rounded. The only fixed trash control device at each port is a single, well-rounded, vertical, concrete trash bar located midway across the intake. The elephant trunk intake is flared at the entrance with a curved, concrete trashrack. The dimensions of the intake are about 20 ft tall by 30 ft wide. However, the intake conduit transitions to smaller dimensions for smooth passage of flow through the existing 8- by 15-ft port at the wet well face.

9. Releases from the wet well are made primarily through the hydropower facilities. Hydropower flows pass through a penstock intake in the wet well at invert el 1,690. The maximum hydropower discharge is about 2,400 cfs.* The capacity of the hydropower system is often exceeded by the total project discharge. Excess flows normally pass through the regulating outlet (RO).

* Personal communication, 28 August 1986, with Mr. R. A. Cassidy, Environmental Engineer, US Army Engineer District, Portland, Portland, OR.

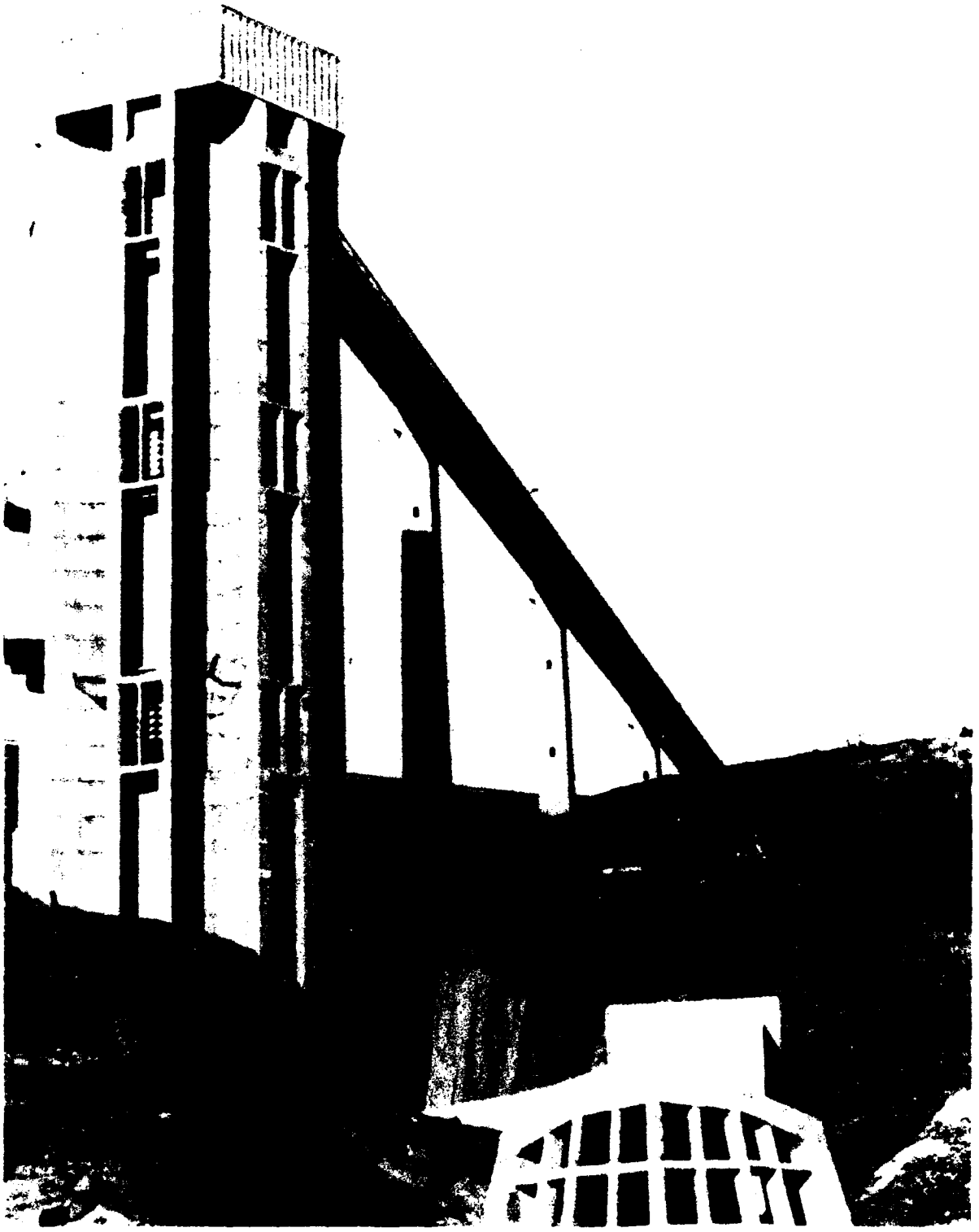

Figure 3. Lost Creek Dam intake structure

This outlet from the wet well consists of a pair of rectangular passages with invert elevations of 1,640, which transition into a single, circular conduit. This conduit leads to an energy-dissipating flip bucket stilling basin downstream. The Portland District operates the intake structure on the basis of a maximum flow of 11,500 cfs.

10. While the operation of this intake structure is concerned with maintaining the in-reservoir water quality, its primary goal is the maintenance of downstream water quality. The Rogue River, several miles downstream of the Lost Creek Dam, has been declared a wild and scenic river as shown in Figure 1. The river is internationally known for its anadromous fishery, which has been valued at $31.5 million annually (Cramer et al. 1985). In conjunction with the Lost Creek Dam, the US Army Corps of Engineers built a fish hatchery and a fish barrier dam a little downstream of the main dam to prevent fish passage into the tailrace and the turbines.

The Problem

11. The environment in the Rogue River downstream of the dam is very sensitive to water temperature, especially the fishery. Biological mechanisms in anadromous fish that control the development rates of eggs and young fish are thought to be very dependent on water temperature (Cramer et al. 1985). As the Rogue River is impounded only by irrigation diversion structures between the Lost Creek Dam and the Pacific Ocean (158 river miles downstream), the impacts of the release water temperature from Lost Creek Dam on the riverine temperature downstream are potentially significant.

12. The release water temperature from Lost Creek is regulated to a large extent through the use of selective withdrawal. This is a method of withdrawing water from a specific vertical range within the reservoir to meet a prescribed downstream release quality objective. This method uses density strata within the reservoir that correspond, most commonly in freshwater bodies, to horizontally oriented temperature strata. Temperature stratification, more prevalent in the warmer months of the year, results primarily from the influx of heat across the water surface. The surface waters of a reservoir capture much of the incoming heat, become lighter, and therefore, more easily buoyed. These waters then tend to remain at the surface where they can accept more heat and become even lighter. The bottom waters, especially in a

reservoir as deep as Lost Creek, do not receive much of the heat influx. Therefore, they remain cooler and more dense. Density stratification of this sort is self-maintaining throughout the warmer months in that vertical transport of water and resulting thermal mixing are greatly inhibited by the stratification itself. The reduced vertical transport also often permits the development of tratification of other water quality constituents, making selective withdrawal even more important in downstream water quality maintenance. In the fall, stratification breaks up at many reservoirs when the surface waters are cooled and the flows are larger. The cooling promotes convective mixing and the higher flows contribute to advective mixing.

13. The Oregon Department of Fish and Wildlife and the Portland District have jointly developed release target temperature guidance designed to minimize adverse temperature impacts to the anadromous fishery downstream. Since construction completion, the Portland District has operated on the basis of using the best available guidance at the time to decide which intakes should be opene' to release the required temperature of water.

14. The uniqueness of the intake structure has posed some complexities in operation. All the intakes enter the same wet well. When more than one level of intakes is operated simultaneously, the density stratification within the reservoir can impact the flow distribution between those port levels compared to the flow distribution with homogeneous density conditions (Howington 1988). This, in turn, can influence the release temperature. Operations at the structure presently employ more than one level of intakes simultaneously, those operating being chosen based on dam operator experience. The port selection is checked by measurement of the temperature downstream and comparison to the temperature target. If the two do not correspond adequately, the port selections may be changed.

15. The type of operation described has generally been adequate in meeting the desired release targets much of the year. However, in the late fall, winter, and early spring, the release temperatures have been consistently warmer than the temperature targets. Changing operations during these periods has been found to provide little or no improvement in the release temperatures because the desired release temperatures either do not exist within the pool or cannot be accessed by the selective withdrawal system.

16. These warm release temperatures are thought to result in earlier-than-desirable emergence of the fish downstream (Cramer et al. 1985). The

very young fish (fry) are emerging from the eggs (redds) in the streambed gravel prior to development of an adequate food supply. It was thought that if release temperatures could be reduced during these critical periods by a reallocation of the coolwater resources in the Lost Creek Lake, this early emergence problem might be reduced and a higher survival rate among the fry attained (Cramer et al. 1985).

The study objectives

17. A study was undertaken by the US Army Engineer Waterways Experiment Station (WES) to evaluate thoroughly the withdrawal characteristics of the intake structure to produce a better means of operating the structure to meet release temperature targets on a yearly basis. One goal was to develop a method of daily operation that would be less dependent upon operator experience and eliminate the need for hit-or-miss port selection during which the downstream environment might be subjected to abrupt temperature changes while the proper gate selection was being attained.

18. The study was also designed to evaluate the potential for modifying the yearly operational temperature target strategy. These modifications could provide a plan for releasing water warmer than desirable during the less critical periods of the year to conserve the cool water for release during the highly critical periods for the downstream fishery. This alternate operational pattern would, in theory, produce the allocation of the limited coolwater resource that would be most environmentally beneficial downstream.

Scope of the study

19. To perform these evaluations, a scaled physical model coupled with a mathematical model was used. The physical model was used to characterize the withdrawal from the structure for varying physical conditions. The mathematical model was used to evaluate operational alternatives based upon the withdrawal description from the physical model work.

PART II: SELECTIVE WITHDRAWAL

Background

20. As described previously, selective withdrawal (Bohan and Grace 1973, Smith et al. 1987) is a widely used technique for in-reservoir and/or release water quality maintenance. Density stratification acts to vertically confine the region from which water is withdrawn in the reservoir, thereby allowing the selection and release of a partially controllable quality of water when the discharge, withdrawal device characteristics, and in-reservoir resource availability permit.

21. It has been substantiated that most reservoir intake structure ports, although consisting often of considerable area, usually act as point sinks in a reservoir (Smith et al. 1987). A significant body of work exists on the behavior of these assumed point sinks in a vertically density stratified fluid such as a thermally stratified reservoir. The withdrawal of water through these types of ports from a stratified reservoir produces, at some distance away from the intake port, an essentially unidirectional velocity profile in the longitudinal-vertical plane as seen in Figure 4. This velocity profile, whose size and shape depend substantially on the stratification pattern in the fluid, can be used to predict the contribution made by any

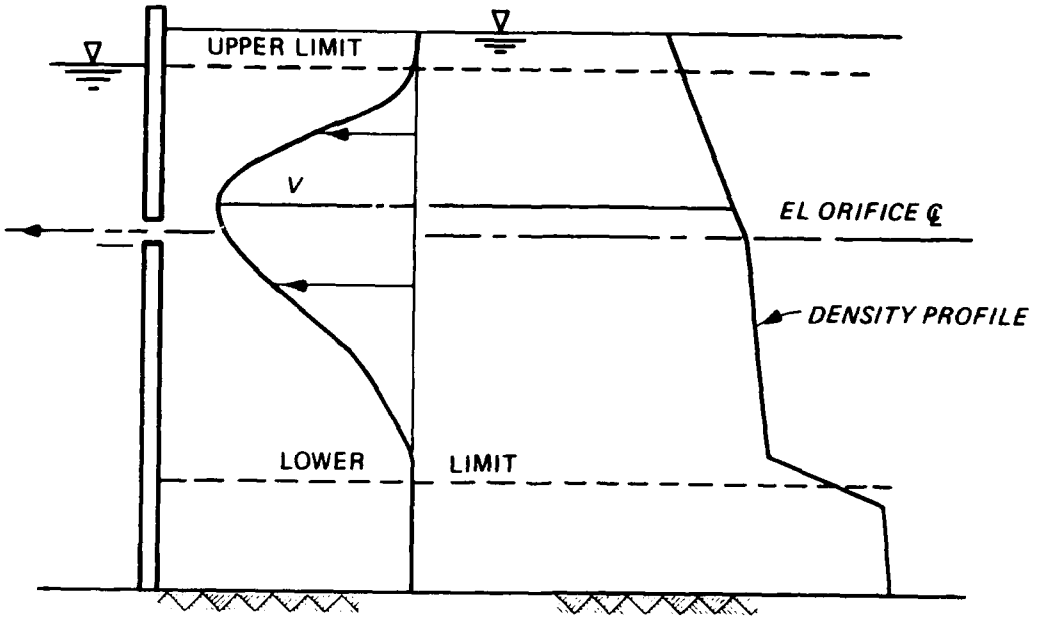

Figure 4. Example vertical velocity profile

horizontally oriented reservoir stratum to the withdrawn water quantity. This knowledge leads directly to the prediction of release water quality characteristics such as density, temperature, and other stratified water quality components given a known vertical profile for these components.

22. Bohan and Grace (1973) proposed methods for relating the size and shape of the velocity profile to density stratification and flow rate through the intake port (two normally obtainable pieces of information). This yielded a means of predicting the release water quality characteristics from a port by simply knowing the vertical distributions of the water density and the desired water quality constituent, the port elevation, and the discharge. Equation 1, developed by Bohan and Grace, permitted computation of the upper and lower limits of withdrawal that described the vertical extent of the velocity profile generated by the port operation:

$$\frac{Q}{Z^3\sqrt{\frac{g}{Z}\frac{\Delta\rho}{\rho}}} = 1.0 \qquad (1)$$

where

Q = flow rate, cfs

Z = elevation difference between the port center line and the upper or lower limit of withdrawal, ft

g = gravitational acceleration, ft/sec^2

$\Delta\rho$ = fluid density difference between the port center line and the upper or lower limit of withdrawal, pcf

ρ = fluid density at the port center line, pcf

23. This approach was later found to have applicability only for those withdrawal zones (vertical range between the limits of withdrawal) that did not intersect either the water surface (upper boundary) or the reservoir bottom (lower boundary). Equation 1 was also found to be less accurate for those ports with near-field topography unlike the original test conditions, which consisted of an orifice in a vertical, flat plate. The description for selective withdrawal has since been updated to account for both boundary interference and near-field topographic influences. The most recent selective withdrawal equations for orifice flow from Smith et al. (1987) are given, in simplest form, by

$$\frac{Q}{Z^3\sqrt{\frac{g}{Z}\frac{\Delta\rho}{\rho}}} = \frac{\theta}{\pi} \tag{2}$$

$$\frac{Q}{D^3\sqrt{\frac{g}{D}\frac{\Delta\rho}{\rho}}} = \frac{\theta}{2\pi}\,\frac{1 + \frac{1}{\pi}\sin\left(\frac{\frac{b}{D}}{1 - \frac{b}{D}}\,\pi\right) + \frac{\frac{b}{D}}{1\,\frac{b}{D}}}{\left(1 + \frac{\frac{b}{D}}{1 - \frac{b}{D}}\right)^3} \tag{3}$$

where

$\Delta\rho$ = fluid density difference between the boundary of interference and the free limit of withdrawal, pcf

θ = effective angle of withdrawal, rad

π = pi (3.14159), rad

D = distance between the boundary of interference and the free limit of withdrawal, ft

b = distance between the center line of the outlet and the free limit of withdrawal, ft

24. Equation 2 is used when no boundary interference occurs while Equation 3 applies to the boundary interference problem. The effective angle of withdrawal θ in both Equations 2 and 3 is the means by which the descriptions account for simple, localized topographic influences. A completely unobstructed intake, closely approximated by a vertical pipe in the center of a deep water body, would withdraw water from 360 deg (2π rad) in plan view. The effect of these topographic influences is to confine the withdrawal zone laterally, resulting in a vertical expansion of the withdrawal zone compared to the completely unobstructed intake.

25. The physical significance of the effective angle of withdrawal is easily seen in a few test cases. For an orifice in a semi-infinite flat plate, the value of θ was found to equal about 3.14 rad or about 180 deg. Research on ports mounted in a 90-deg corner at the meeting of two vertical flat plates confirmed that the θ value was, indeed, about 1.57 rad (Smith et al. 1987). Essentially, if the withdrawal zone is laterally confined, it will expand vertically to compensate. Therefore, the inclusion of the effective angle of withdrawal has provided an amount of pseudomultidimensionality to the selective withdrawal description.

26. The shape of the in-reservoir velocity profile produced by port operation has been predicted based purely on empirical descriptions. A set of these descriptions was developed by Bohan and Grace (1973) and is given in Equations 4 and 5.

$$\frac{v}{V} = \left(1 - \frac{y\Delta\rho}{Y\Delta\rho_m}\right)^2 \tag{4}$$

$$\frac{y_1}{H} = \left[\sin\left(1.57 * \frac{z_1}{H}\right)\right]^2 \tag{5}$$

where

v = local velocity, fps

V = maximum velocity, fps

y = distance between the center line of the port and the point of interest, ft

$\Delta\rho$ = fluid density difference between the center line of the port and the point of interest, pcf

Y = distance between the center line of the port and the free limit, ft

$\Delta\rho_m$ = fluid density difference between the center line of the port and the free limit, pcf

y_1 = distance between the elevation of maximum velocity and the lower limit of withdrawal, ft

H = thickness of the withdrawal zone, ft

z_1 = distance between the center-line elevation of the port and the lower limit of withdrawal, ft

Equation 4 relates the vertical position within the withdrawal zone and the density gradient to the relative velocities within the velocity profile. The location of the maximum velocity is predicted through the empirical description in Equation 5.

27. In general, adequate research has been done to estimate confidently the withdrawal velocity profile, and thereby the release water quality characteristics, for traditional intake structures with simple near-field topography. However, for structures such as that at Lost Creek, the influences of the unique near-field topography could not be accurately estimated with the generalized techniques. Therefore, the use of a three-dimensional physical

model was required for determination of the characteristics of the withdrawal patterns. Prototype testing to determine these influences was not a practical alternative to a physical model since many stratification and flow conditions needed to be tested, requiring multiple visits to the project over an extended time period.

Intake Structure Physical Model

28. An operating scale model of the Lost Creek Dam intake structure was constructed to evaluate the characteristics of selective withdrawal and simultaneous multiple level withdrawal (more commonly known as blending). The model scale selected was 1 ft in the model equaling 80 ft in the prototype. The criterion for establishing this model size was primarily flume size. The tallest available flume for selective withdrawal modeling was 4 ft tall. Since a minimum prototype length of about 305 ft vertically needed to be reproduced, the scale selected was 1:80. This scaling corresponded well with previous selective withdrawal work, which had been performed in physical models with scales normally ranging from 1:40 to 1:100. The 1:80 scale was adequate for these types of tests as in-structure hydrodynamics were not being evaluated. The modeling revolved around mixing that has traditionally been reproducible at these scales.

Froude number scaling

29. The scaling procedure for these types of models is based on Froude ratio similitude. The scaling of model parameters is such that the Froude number, the ratio of inertial to gravitational forces, remains the same between the model and the prototype. This results in a length scaling that is equal to the established model scale. The resulting scaling parameters follow:

$$R * L_m = L_p$$

$$R^{0.5} * V_m = V_p$$

$$R^{2.5} * Q_m = Q_p$$

$$\Delta\rho_m = \Delta\rho_p$$

where

R = general model scale (in this case, 80)

L_m, L_p = length in the model and prototype

V_m, V_p = velocity in the model and prototype

Q_m, Q_p = flow rate in the model and prototype

$\Delta\rho_m$, $\Delta\rho_p$ = density differences in the model and prototype

30. Scaling of the Lost Creek model resulted in a maximum model flow rate of 90.2 gpm, which corresponds to the 11,500-cfs maximum imposed on the prototype structure. Tests conducted at this maximum discharge in the original flume would have experienced an unacceptably high drawdown of the simulated lake level in excess of 0.15 model feet during the shortest possible testing period of about 10 min. Since it is generally not possible to replenish stratified fluid during a test without disturbing the stratification patterns significantly, each test must rely entirely on the stored volume in the simulated reservoir. For this reason, and to minimize the drawdown at more commonly used discharges, the surface area and volume of the flume were expanded as seen in Figure 5.

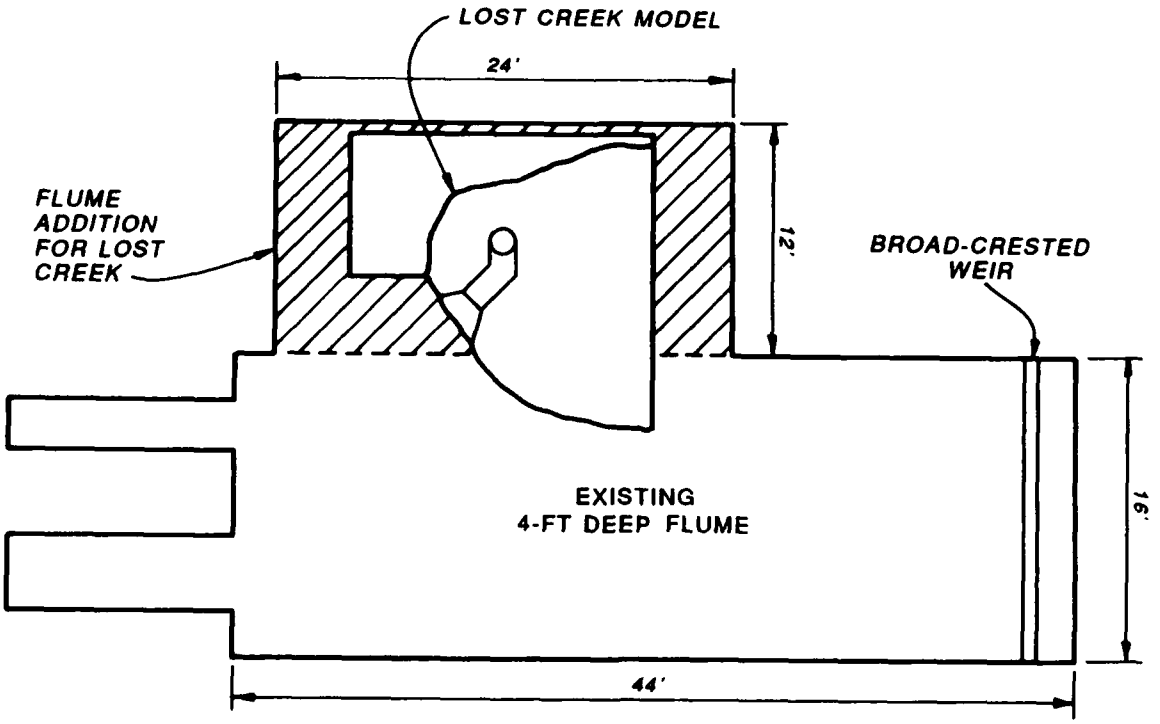

Figure 5. Plan view of the test flume

Intake model features

31. The 1:80-scale Plexiglas model of the intake structure is a detailed replica of the prototype structure with individually operable intake ports. Special care was taken to represent the curvature of the intake edges including the rounded trash bar at the entrance to each intake. The turbidity intake was also modeled. Both the regulating outlet and the hydropower outlet from the wet well were carefully reproduced. Such attention to detail within the wet well of the structure is not common in selective withdrawal modeling. However, it was required because the evaluation of blending might have been influenced by the wet well geometry and details.

32. The near-field topography in the vicinity of the intake structure was modeled to assess accurately its impact on selective withdrawal characteristics. Previous selective withdrawal work had indicated that the topographic influences were limited laterally to twice the withdrawal zone thickness in any direction. Since the maximum withdrawal zone thickness cannot exceed the maximum pool depth, the topography needed to be modeled outward about twice the maximum depth, or about 8 model feet.

33. The dam face was represented in the model with marine plywood. However, to simulate the hillside and excavations housing the intake structure, a more three-dimensional medium was desired. A base platform system was constructed of wood on which metal templates were affixed. Sand was then added to near the top of the templates. A thin layer of fine-aggregate concrete was then placed on the sand to complete the hillside. The floors of the excavations were flat and were pieced in with plywood. The resulting physical model is shown in Figure 6.

Model flow measurement

34. Separate polyvinyl chloride (PVC) piping was placed under the topography to permit releases through the regulating outlet and the hydropower outlet. These pipes were spliced through the wall of the Plexiglas flume and extended down to the floor level and into a series of rotameter flow measuring devices. These devices measure flow based on the vertical position of a weight with known drag characteristics. The weight was placed in a conical glass tube and was pushed upward by the passing flow. The position of the weight was calibrated against the flow rate through the device. For this model, six rotameters ranging in maximum capacity from 4.5 to 40 gpm were employed. Three each were used for the hydropower and the regulating outlet

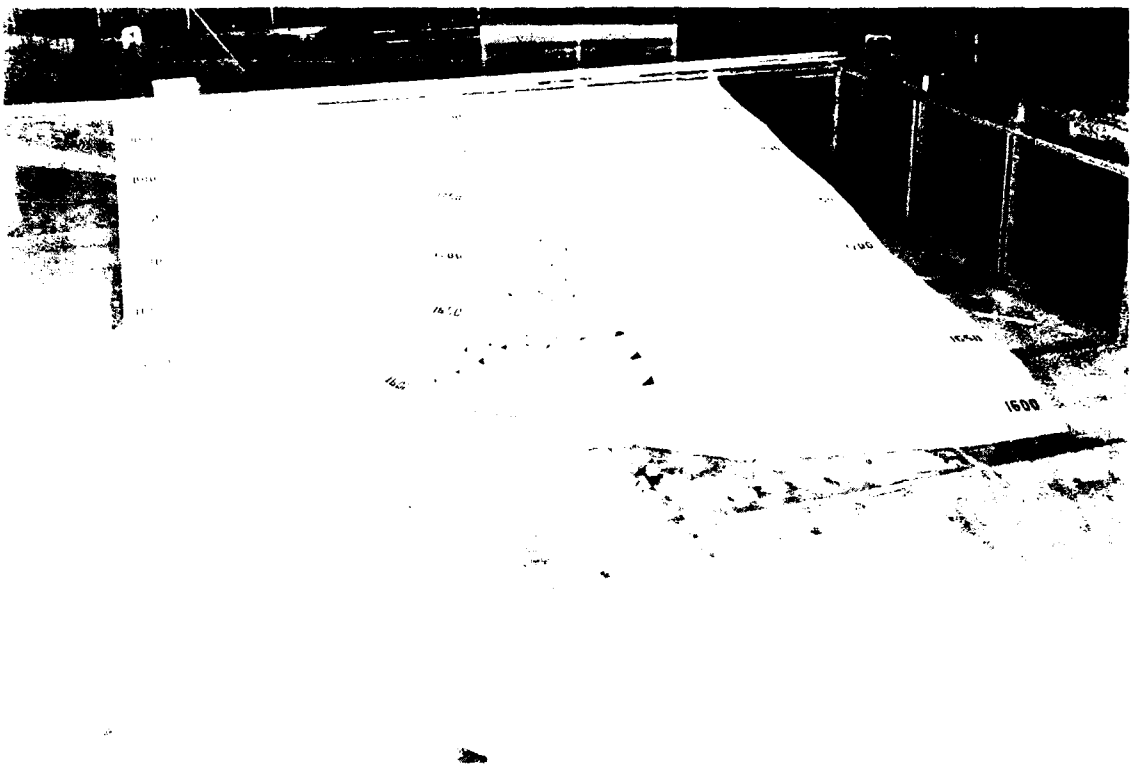

Figure 6. 1:80 physical model of intake structure

discharge measurements. Downstream of the rotameters were flow control gate valves, and below them, an outlet trough. Flow from the model was gravity driven at all times.

Testing procedures

35. Density stratification within the lake normally resulting from temperature stratification was simulated in the model through salinity. This technique created absolute water densities slightly greater than 62.4 pcf rather than slightly less, as experienced in the prototype. This difference has proven to be permissible since maintenance of densimetric Froude number similitude between model and prototype is significantly more dependent upon the accurate representation of the density differences rather than absolute water densities. This stems from the division of absolute density into density difference within the computation of densimetric Froude number and the very small variation in densities encountered in this type of stratified flow modeling (usually less than 0.5 percent change in density).

36. Food-grade salt was added to the water in the flume in varying amounts increasing with depth to produce density strata. This effect was achieved by filling the flume slowly in layers. The most highly saline

waters, which represented the hypolimnion of the reservoir, were put in the flume first. Then, the epilimnion, represented by a freshwater layer, was added. A broad-crested weir was used to inhibit mixing and smearing of the density interface. The stratification pattern was often manipulated at this point by localized mixing from small submersible pumps to represent more closely a stratification pattern found in the prototype. The density patterns seen in the prototype could not be replicated exactly as diffusive mixing and mixing from surface stress could not be completely controlled in the model. Mixing due to surface stress was greatly reduced in the model by covering the flume with plastic sheeting. Similarity between the model and prototype density patterns was desired, but exact replication was not necessary since multiple density patterns that banded those observed in the prototype were simulated.

37. Once the flume was filled and the stratification was deemed acceptable, the model pool was allowed to stabilize; that is, the currents remaining from the filling and stratification process were allowed to subside. Crystalline dye was usually dropped into the flume to observe the magnitude of the extraneous currents. After the currents had calmed, the density stratification pattern was more accurately measured. First, three samples were extracted from the model pool. These usually represented a surface, a median, and a bottom sample. These samples served to relate measurable conductivity and temperature of the samples to known densities. In situ fluid density could then be computed from measurement of temperature and conductivity within the pool. The densities of the samples were measured using a hydrometer. The conductivities and temperatures of the samples were then measured. These tasks were accomplished in the first few selective withdrawal tests using a Digitec temperature probe and Beckman specific conductance meter. This arrangement was particularly difficult to move and to use and was replaced by a Yellow Springs Instruments (YSI) Model 32FL field conductivity and temperature meter. The probes used were a model 3417 plastic-encased YSI conductivity cell and a 700-series YSI temperature probe.

38. The probes were attached to a fixed point gage. This arrangement provided a way of measuring the vertical location of the probes accurately. The probes were then lowered through the pool depth at small intervals (usually 0.1 ft through the significant gradients and 0.2 ft otherwise) and the temperature and conductivity were measured. Care was exercised to ensure

that the measurement intervals were small enough to describe adequately any sharp density gradients. The resulting values produced a density profile based on the sample measurements. This process was performed only at one plan view location as the pool was assumed to be homogeneous both laterally and longitudinally. Given the lengthy settling period and the care taken in setting up the model, this was a valid assumption. All of the preceding steps were performed prior to releasing any flow through the model.

39. The actual testing was then begun. The selected port or ports at the face of the structure were then secured open. One or more of the flow-controlling gate valves at the rotameters were opened until the desired flow registered on the rotameters. The system was then allowed to reach a pseudo-equilibrium state. An actual equilibrium was not possible as the water surface was slowly dropping and the stratification pattern was slowly changing, but neither changed significantly during a single test. This was ensured under high-flow conditions by limiting the length of each test to a maximum of 10 min. Reaching this stabilized state usually required only a few minutes.

40. It was then assumed that a steady velocity profile had developed within the pool. To detect this profile, crystalline dye was again dropped. This type of dye left a thin, vertical streak of dyed water that was easily tracked. The dye was dropped far enough away from the intake structure so that the flow was virtually unidirectional (longitudinal). The dye streak was dropped in front of a fixed grid for vertical reference, and the streak displacement was filmed through the transparent flume walls by a tripod-mounted video camera located at about the elevation of the open intake port. A video monitor and video cassette recorder were employed to record the dye streak. Experience had indicated that the fixed grid must be located on a radial line from the intake port to cause the least interference with the flow field established by releases through that port. Each test continued, up to the maximum of 10 min, until the dye streak had developed a clear profile with discernible limits of withdrawal.

Data reduction

41. After each test, the recorded dye streak was transferred to paper by hand tracing. The profile was then converted to a series of elevations and normalized velocities (i.e., velocities relative to the maximum velocity in the profile). The tracing of the velocity profile was placed on a plotter bed, which was used as a graphics input tablet. This allowed the computer to

accept a series of inputs from the plotter and produce a small data file approximately describing the velocity profile. The conductivity and temperature profile information, the flow rate, the intake port openings, and other pertinent information were entered into a separate data file. These two data files were then accessed by a computer code that produced a density profile, computed the maximum velocity elevation and related shape information from the observed profile, and, based on the observed limits of withdrawal and Equation 2, computed an effective angle of withdrawal for each free withdrawal limit. Graphical representation of the results were produced as seen in the example in Figure 7. This figure shows the observed density stratification, the shape of the observed velocity profile, the open port, the flow rate, and the computed effective angle(s) of withdrawal θ .

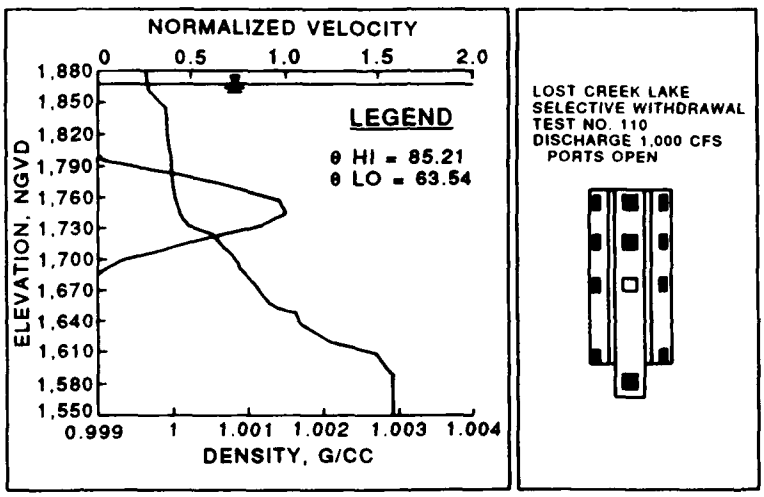

Figure 7. Sample graphical output from selective withdrawal testing

Selective Withdrawal Test Results

42. Each intermediate flow test (those experiencing no boundary interference) produced two values of effective angle of withdrawal (one for each limit), one point of maximum velocity, and about eight to ten points describing the shape of the profile. Each test with only one free limit (either the surface or the bottom boundary was intersected by the withdrawal profile, but not both) produced one value for effective angle of withdrawal, no pertinent maximum velocity elevation data, and about five points describing the velocity profile shape. The utility of the tests with one boundary of interference was limited by the inability to identify, during testing, the theoretical limit of

withdrawal located outside the pool. The theoretical limit is the elevation that would describe the withdrawal limit, were not the interfering boundary encountered. Since much of the shape description, maximum velocity elevation, and one of the two effective angles of withdrawal are recorded with reference to this immeasurable limit, they could not be included in the data reduction.

Withdrawal angle

43. The results of the Lost Creek model testing for withdrawal angle are tabulated in Appendix A. Comparison of the data indicated no trends in the differences in withdrawal angle among ports at the same port level. The observed differences were attributed to measurement errors during model testing. Therefore, the data were grouped by port level. The averaged values for the five port levels are given in the following tabulation. No significant variation in these values was observed with discharge.

Port Level	Center-line El	Effective Angle of Withdrawal	
		Deg	Rad
1	1,852.5	177	3.09
2	1,797.5	141	2.45
3	1,737.5	80	1.40
4	1,647.5	62	1.08
5	1,603.0	85	1.48

44. Port level 3 has a center-line elevation of 1,737.5. In the majority of tests conducted at this port level, both limits of withdrawal were located within the pool. The effective angle of withdrawal computed from the upper limit was consistently somewhat larger than that computed using the lower limit. This trend could be attributed to the topography. The ports at level 3 were located slightly above the original hillside elevation. The excavation for construction of the intake structure was located immediately below and in front of the ports. The effect of the excavation was to confine the lower portion of the withdrawal zone, thereby yielding a smaller effective withdrawal angle than was produced by the relatively unconfined upper portion of the withdrawal zone. The difference between the two computed angles, although generally consistently present, was too small to produce significantly different limits than an average of the two values. Therefore, a dual-angle approach for computing the effective angle of withdrawal at this port level was considered unnecessary and the average value was accepted.

45. The variability of the computed effective angles of withdrawal among ports at the same elevation, or even the same port for different tests, was found to be insignificant for this study. The relation between the size of the withdrawal zone and the effective angle of withdrawal is cubic in nature. Therefore, a large deviation in effective angle of withdrawal produces a small deviation in withdrawal zone thickness. Further, the agreement among the withdrawal angle test results from Lost Creek is actually quite good. Therefore, the impacts of this observed variability were inconsequential.

46. A demonstration of the accuracy of the prediction capabilities of selective withdrawal technology can be found in Figure 8. Ten tests were selected from the 35 successful tests conducted. Two tests from each of the five levels were selected at random. The averaged effective angles of withdrawal from the tabulation in paragraph 43 were used in the selective withdrawal model, SELECT (Davis et al. 1987), to predict the elevations of the limits. As can be seen in the figure, although the scatter among the observed angles appeared large, the impact of this scatter on predictive capability was small.

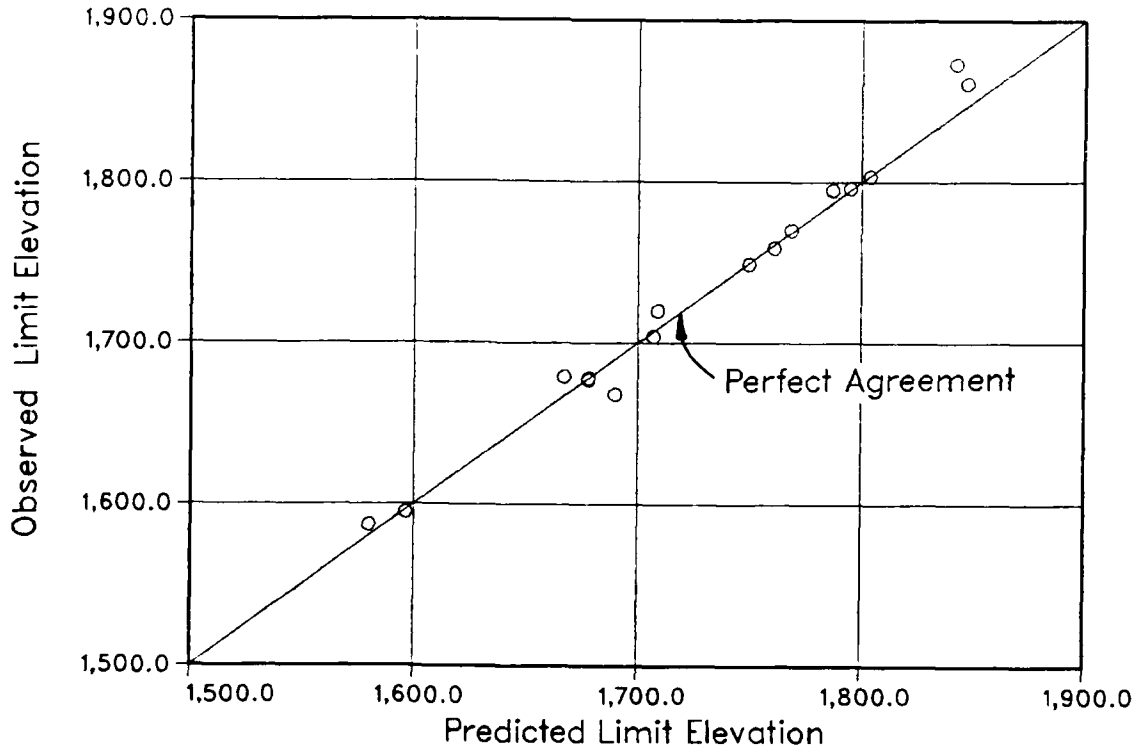

Figure 8. Predicted versus observed limits of withdrawal

Velocity profile shape

47. Upon completion of data reduction for each individual selective withdrawal test, a data base was available for the evaluation of the shape of the velocity profiles. Each test evaluation produced a small data file containing normalized velocities, fractions of withdrawal zone thicknesses, and incremental density differences. These data were concatenated into a single data file and statistically compared to previous selective withdrawal work. The comparison can be seen in Figure 9. The line represents the shape function determined by Bohan and Grace (1973). Although the data scatter was significant, the existing theory appeared to provide an appropriate fit of the observed data. The data scatter was probably due, for the most part, to sharp density gradients in the pool. An inherent assumption in the shape function equation is that the density gradient is piecewise-linear between the center line of the port and any point along the velocity profile. This assumption, although not always accurate, generally produces acceptable predicted normalized velocity profiles. The results of this analysis indicated that the existing description for profile shape should be retained.

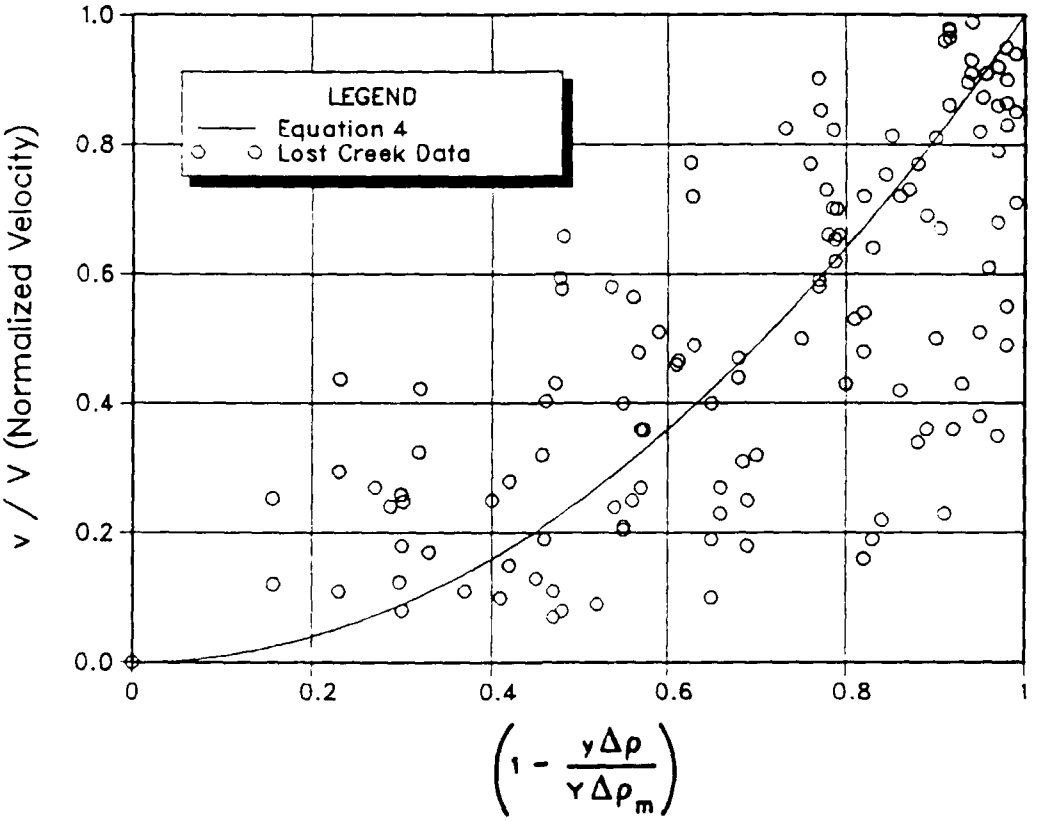

Figure 9. Normalized velocity profile shape evaluation

Maximum velocity location

48. The elevation of maximum velocity has been empirically related to the withdrawal limits and the port center-line elevation by Equation 5. The Lost Creek Lake selective withdrawal evaluation produced 14 data points with which to evaluate this description. The Lost Creek data, as seen in Figure 10, did not provide definitive proof that the description was accurate since the data were confined to a narrow band. The remaining symbols in the plot represent the original data collected by Bohan and Grace (1973), from which the description was developed. Based upon good correlation between the Lost Creek results and the original Bohan and Grace results, the existing empirical description for maximum velocity location was also retained.

Summary

49. In general, the selective withdrawal results from the Lost Creek model study were very supportive of the existing selective withdrawal technology. The resulting effective angles of withdrawal seemed to follow closely the patterns established in earlier work. The velocity profile descriptions, including shape and maximum velocity elevation, also blended well with previous results. This conformity with the concepts of the existing technology

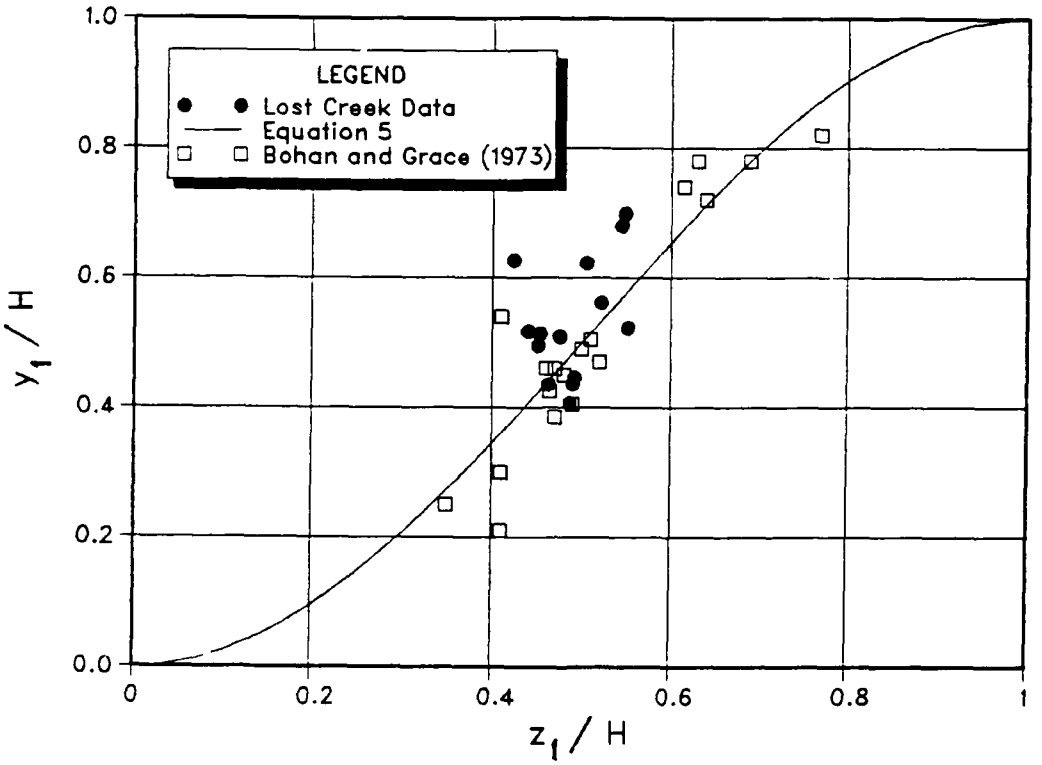

Figure 10. Maximum velocity elevation evaluation

both increased the confidence in the applicability of the generalized selective withdrawal concept and enhanced the credibility of the results from this particular evaluation.

PART III: SIMULTANEOUS MULTILEVEL WITHDRAWAL

50. At Lost Creek Lake, as at many US Army Corps of Engineer impoundments, there are stringent requirements on release water temperature. For this reason, use of a single level of intake ports at any one time may not be adequate. However, as previously mentioned, the use of multiple intakes in a single wet well structure such as Lost Creek is influenced by density stratification. The pool density pattern may significantly affect the flow distribution between the withdrawal levels, thereby affecting the release water temperature. The evaluation of this pattern, discussed in the following paragraphs, was designed to provide a means of predicting these density influences and to produce operational guidance that would make structure operation less dependent on operator experience alone.

Concurrently Developed Theory

51. Research in the area of simultaneous multilevel withdrawal from stratified reservoirs (blending) was conducted concurrently with the Lost Creek study (Howington, in preparation). As discovered in this work, density influences on port flow distribution can be significant. In the most severe case, flow through one or more open ports may be effectively blocked by the buoyant forces associated with different water densities, hence the term buoyancy blockage. This situation, most commonly associated with strong stratification and low discharge, occurs when the hydraulic losses incurred by flow entering the wet well are insufficient to overcome the potential energy of the density differences between the pool and the wet well. When the two opposing components, hydraulic losses and buoyancy, are equal, the system is at a critical equilibrium. The discharge at which this equilibrium occurs is known as critical discharge. Any discharge greater than critical discharge will induce flow through the previously blocked port, but the distribution of flow among the open ports may still be significantly different from that expected in a homogeneous environment.

52. An algorithm produced during the research on simultaneous multilevel withdrawal was employed in the analysis of the Lost Creek blending data. This stratified-flow-distribution (blending) algorithm provided a method of computing the individual port flows based upon the total discharge, intake

port elevations, a description of the individual port head loss coefficients (which were developed for this study during the unstratified flow testing), and a quantified buoyancy head term at each open port level that described the amount of potential energy due to stratification influencing the flow distribution.

Algorithm Modifications for Lost Creek Application

53. Previous research in this area had allowed the density influences (represented through the buoyancy head) to be computed as seen in Figure 11a for three levels of simultaneous withdrawal (Howington 1988). The buoyancy head is really a measure of the additional potential energy due to stratification available at a port level. The buoyancy head for each level is cumulative proceeding downward. A positive density influence (a positive buoyancy head) for a level indicates that the stratification-influenced flow distribution will favor that level compared to homogeneous density distribution. For example, in Figure 11a the buoyancy head on the upper port would be zero. The buoyancy head for the middle port would equal the region labeled "A" divided by the density entering the middle port. That for the lower port would equal the middle-port buoyancy head plus the region B divided by the density entering the lower port. Each region represents the vertical integration of the density difference between the pool and the wet well between the open port levels. This sum corresponds to the total potential energy that must be overcome through hydraulic losses in order to withdraw water from all three levels.

54. The unusual nature of the Lost Creek intake structure forced an extension of the methods used in computing the buoyancy head. This extension was necessary because the outlet devices within the wet well at Lost Creek were not always located below all the intake ports as assumed in the configuration shown in Figure 11a. When only the hydropower outlet was operated, 3 of the 12 ports were located below the outlet, resulting in upward flow within the wet well.

55. The extension of the methods for Lost Creek included accounting for the direction of flow within the wet well. In this manner, the appropriate in-well density is computed and the proper sign on the buoyancy head is produced. The stratification pattern above the wet well outlet produced a

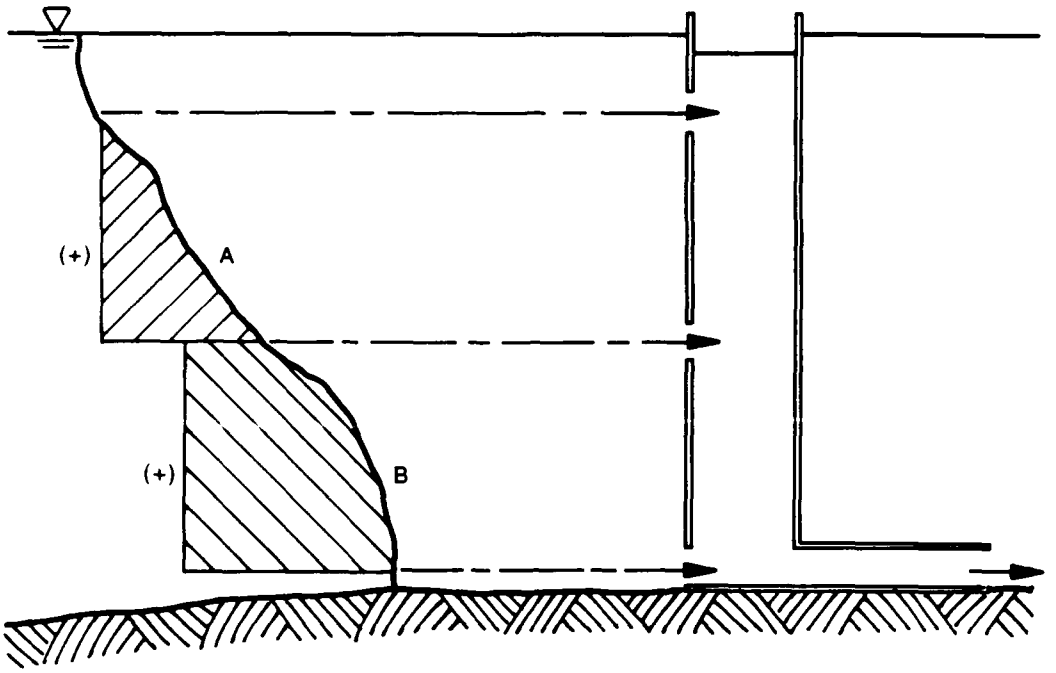

a. More common condition

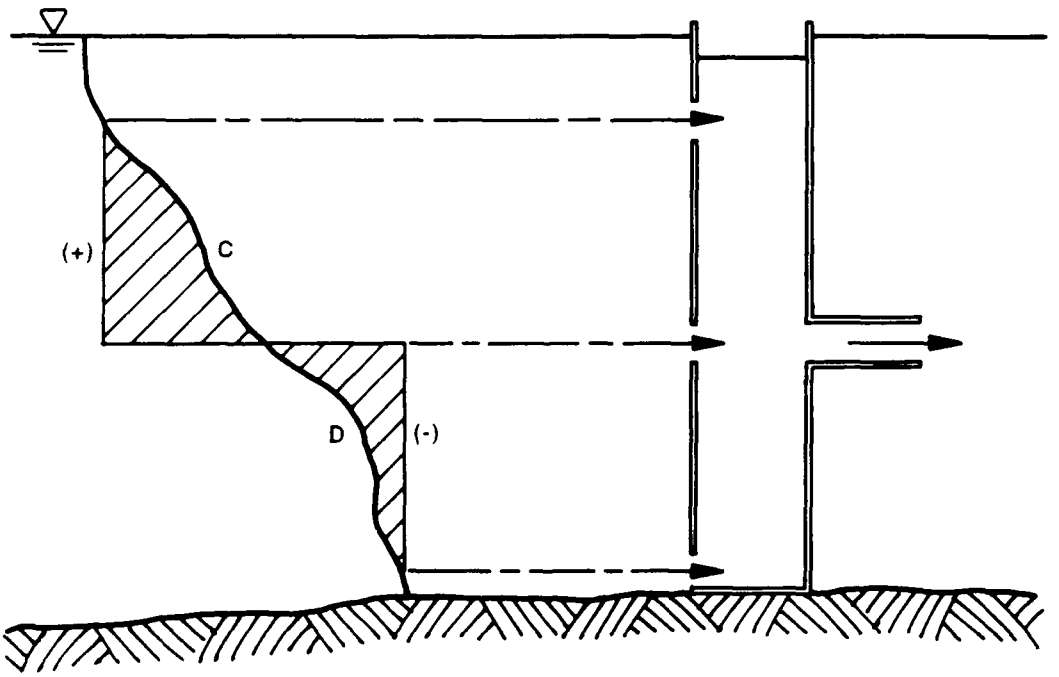

b. Frequent Lost Creek condition

Figure 11. Examples of buoyancy heads with components labeled

positive buoyancy head as seen by region C in Figure 11b. This represented the energy required to "pull" water, which was less dense than the pool water surrounding the wet well, downward within the wet well to the outlet elevation. The reverse was true for the intakes below the wet well outlet. The more dense water had to be pulled upward to the wet well outlet. This resulted in a negative buoyancy head given in Figure 11b by region D. The significance of these terms is that, all else about the ports being equal, the density influences would force the highest percentage of flow through the lowest port in Figure 11a and through the middle port in Figure 11b. The computation of each of these regions was easily performed by approximate graphical integration using a plot of the density profile and a planimeter.

Physical Model Work

56. The physical model of the intake structure described in Part II was also used in the evaluation of simultaneous multilevel withdrawal (blending). Since a purpose of this investigation was to develop the ability to predict flow distributions between elevations, the first order of business was to devise a means of measuring these individual port flows in the model. Conventional methods of port flow measurement were first employed. The ports were individually tapped at the throat of the intake to measure the pressure drop associated with flow through the intake. Tubing led from the structure to a piezometer board outside the model. However, substantial pressure differentials were not observed during testing. Inclination of the piezometer board provided no additional help. The system was enclosed and modified to use two fluids closer in specific weight than air and water. A two-fluid manometer using water and M-3 (Meriam 295) was incorporated. Differentials were measurable with this device, but only at extremely high discharges. Other fluids were sought for use in the manometer, including ethyl acetate, glycerin, and castor oil. None of these provided a stable system for pressure measurement. In many cases, the differentials were adequately large for measurement, but would not produce an adequately stable fluid interface. Maintaining an air bubble-free system also presented difficulty. All attempts to measure pressure differentials accurately using these techniques were unsuccessful.

57. Direct velocity measurement was then considered. Several

alternatives were examined. The method chosen made use of a low-speed propeller-type velocity probe. The device, accompanied by a digital output meter, was manufactured by Nixon Instrumentation, Ltd. The probe consisted of a five-bladed rotor mounted on a stainless steel spindle. The ends of the spindle were conical and rested in jewel bearings. The rotor head was attached to a stainless steel tube that enclosed an insulated gold wire. This tube ended about 0.004 in. from the rotor. The passage of the rotor blades past the gold wire tip modified the impedance between the gold tip and the stainless steel tube, thereby allowing measurement of the rotor's rate of revolution. The low-speed probes used in this study were capable of measuring velocities in the range of 1 to 60 ips. The output from the meter was actually in hertz, but had been factory calibrated; a linear relationship between hertz and velocity was provided with each probe.

58. Velocity, however, was not the intent of the measurement, but a surrogate means of obtaining flow rate. Therefore, the velocity and the discharge had to be related. It was considered impractical to attempt to develop a velocity profile in the immediate vicinity of the intakes and integrate to arrive at discharge since the velocities just away from the port center often became immeasurably small. Further, simple continuity arguments relating discharge, average velocity, and port area were not usable since the velocity measured would not necessarily be an average one. Therefore, it was assumed that, for a fully opened intake port and for the range of flows encountered in the study, the ratio of the velocity to the discharge through the port would remain constant; that is, although the actual velocities would obviously change with the discharge through the port, the velocity-discharge ratio would not.

59. The probes were mounted on point gages for stability during testing. The rotor heads were placed immediately upstream of the ports to be opened and at about the center of the ports vertically. To validate the assumption in the previous paragraph, a wide range of flows were passed through a single open port and the meter readings recorded. The resulting plot of meter reading (linearly related to velocity) and discharge was linear, thereby supporting the assertion that the velocity at that point varied linearly with the flow rate, for the range of flows tested. This knowledge was then used to produce a linear relationship between the meter reading and the discharge through that port. This relationship, however, was not applicable unless the

probe position was maintained exactly. It was then concluded that a new description could be developed through a short series of tests each time the probes were moved. This would essentially calibrate the discharge through that port to the meter reading.

Unstratified flow testing

60. Although the intake sizes and shapes were identical for 11 of the 12 intake ports, the close proximity of some of the intakes to the topography served to produce variation among the levels. When multiple ports are operated in a stratified environment, the flow distribution between these ports will depend on both the hydraulic differences between the ports and the density stratification effects. To discern between these two effects, a sequence of tests was conducted in an unstratified environment to quantify the hydraulic differences between the ports. It should be noted that if each of the intake ports were identical and produced the same head losses for the same flows, this portion of the study would have been unnecessary.

61. Measurement of the hydraulic differences between the ports entailed the development of a relationship between the flow rate and the head loss for each port. Since actual hydraulic losses could not be measured in this model, as evidenced by the extensive manometry work described in the previous section, another method for arriving at these relationships was devised. This method involved the opening of multiple intakes (usually two) in the unstratified pool and the measuring of individual port flows. This procedure was designed to produce a loss relationship among the ports.

62. Tests were conducted to determine if the probe introduced any significant losses. This was done by metering (placing a velocity probe at the port and calibrating it against discharge) one port with two ports open. The flow through the unmetered port was determined by subtracting the metered port flow from the total discharge reading on the rotameters. The same two ports remained open in a second test. However, the probe was moved to the other open port and recalibrated. If the probe were introducing any measurable energy loss, the flow distribution between the two tests would have been different. This, however, was not the case, as the flow distribution was identical for both probe positions (within the measurement accuracy of the instruments).

63. Port 4 (the leftmost port at port level 2, el 1,797.5) was determined to have the smallest hydraulic losses of any of the 12 ports.

It was selected as the "base" port for hydraulic loss analysis. A series of tests were then conducted with port 4 and one other port open. In many of these tests, both open ports were metered and the sum of the measured port flows was verified against the total structure discharge from the rotameters. In later tests, the verification step was omitted and the second port flow was determined by subtraction. Fifty-two unstratified flow tests were conducted. Some were discarded after a posttest calibration of the velocity probes indicated that the point gage mount had probably been moved slightly during these tests.

64. The general format of the tests was to calibrate the velocity probe readings to the discharge through the individual ports, establish the desired port openings, and pass a range of discharges through the structure, usually beginning low and increasing in increments of 1 to 2 gpm. An example of the results of one of these tests is shown in Figure 12. The relationship between total discharge and percentage of total discharge passing through the metered port should be constant in an unstratified environment. However, the trend away from horizontal at the extreme low flows seen in Figure 12 was evident in many of the tests. This might have been caused by slight pool stratification.

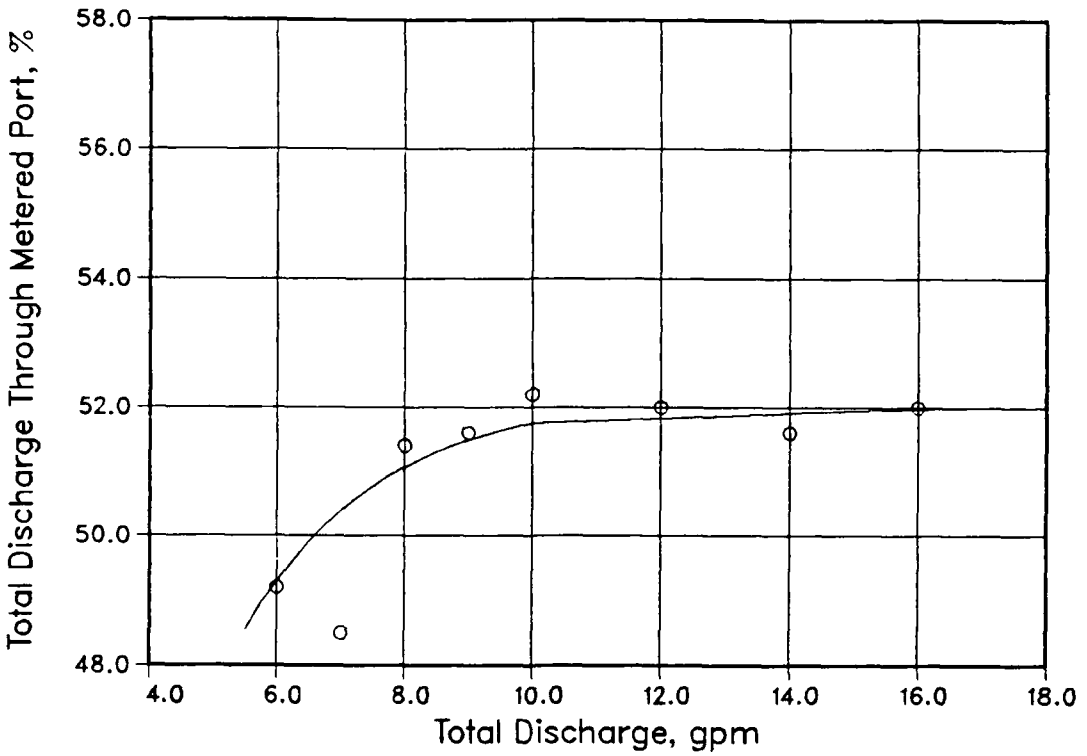

Figure 12. Example of total discharge versus percent through metered port

Although the pool was mixed extensively, some slight stratification, partly thermal, partly saline, was detectable within the pool. Virtually all of the tests produced a clearly constant horizontal relationship for the moderate to higher discharges. For these flows the slight density effects were negated by the magnitude of the hydraulic losses. Thus, the percentage of flow associated with this horizontal line (about 52 percent of total discharge in this figure) was adopted as the flow distribution between these ports for all flows under completely homogeneous conditions since density influences would not then be present.

Hydraulic loss results

65. The results of the tests conducted in a homogeneous density environment can be seen in the following tabulation. Each value represents an average of the percentage distributions of flow for tests conducted for that withdrawal level. The percentage value given for each particular withdrawal level represents the percentage of total discharge that would pass through Port 4 when a port at this level and Port 4 were open in a homogeneous density

Port Level	Center-line El	Percent of Total Discharge Through Port 4 P_4
1	1,852.5	54.5
2	1,797.5	50.0
3	1,737.5	51.5
4	1,647.5	53.8
5	1,603.0	56.5

pool. For example, if Port 7 (at level 3) and Port 4 were open, 51.5 percent of the total discharge would pass through Port 4 and 48.5 percent through Port 7. Although some differences were observed between individual ports at the same port level, these were not significant and were well within the random scatter of the test results.

66. The tests were also geared to evaluate the differences between the operation of the hydropower outlet, the regulating outlet, or both outlets simultaneously. Again, some minor differences were observed, but establishment of a general trend for these differences was not possible as they were small. Therefore, a uniform percentage was established for the flow distribution between port levels relative to the Port 4 level. This percentage was found to be virtually independent of the total discharge, which single port at

that particular port level was open, and the wet well outlet device used.

67. A head loss coefficient for the base port (Port 4) was then estimated. This loss, which is caused by the sudden contraction and a sudden expansion associated with flow passing through the port into the wet well and blending as the flow changes direction once therein, was developed from previous work on orifice and bend losses (US Army Corps of Engineers, Miller 1978). It was estimated that the k coefficient in Equation 6 was about 0.90 for the base port. From this estimation, the remaining port loss coefficients were easily computed from Equations 6 and 7.

$$H_l = \frac{k*V^2}{2*g} \tag{6}$$

$$k_p = k_4 * \left(\frac{P_4}{P_p}\right)^2 \tag{7}$$

where

H_l = head loss, ft

k = head loss coefficient

V = average velocity of the flow entering the port, fps

k_p = head loss coefficient for the port in question

k_4 = head loss coefficient for the base port (4)

P_4 = percentage of flow passing through the base port (4)

P_p = percentage of flow passing through the port in question

68. The following tabulation reflects the application of Equations 6 and 7 to the unstratified flow results. The increased k values for the ports at levels 3 and 4 (compared to level 2) were probably the result of

Port Level	Center-line El	Loss Coefficient k_p
1	1,852.5	1.29
2	1,797.5	.0.90
3	1,737.5	1.02
4	1,647.5	1.22
5	1,603.0	1.52

topographic influences. The high value at port level 1 was probably the result of water-surface influences. The head loss coefficient for level 1 may, therefore, have been depth dependent. However, the range of potential water-surface elevations between the maximum pool elevation and the minimum pool for adequate submergence on level 1 was very small, eliminating the need to examine this possibility for most operations. Port level 5 had a high loss coefficient because of the additional losses associated with flow passage through the elephant trunk. The percentages in this tabulation indicate that, in the absence of stratification, the flow distribution does not stray significantly from equal flow through each of the open intakes, which is what would be expected if all aspects of the ports were identical. However, the differences, although small, do warrant inclusion in the blending description. Since the computed loss coefficients were ultimately dependent on the estimated value of the port 4 coefficient, a sensitivity analysis was conducted to examine the effect of modifying this coefficient. The port 4 loss coefficient was varied between 0.7 and 1.1 and the other levels were computed as shown in Equations 6 and 7. The effect on flow distribution was minor as long as the ratio among the loss coefficients was constant. The best agreement between predictions and observations occurred at the originally estimated 0.9 value.

Stratified pool testing

69. When the influences of hydraulic characteristics for each port on flow distribution among the ports were known, the quantification of the density stratification impacts could be performed by testing in a stratified pool. These tests were conducted much as the unstratified tests except that the density stratification determination was additionally necessary. Density stratification was determined exactly as in the selective withdrawal testing (see paragraph 37). Approximately 38 tests were conducted during this portion of the study. The number of ports open at one time ranged from two to five and the number of levels of simultaneous withdrawal ranged from two to four. The stratification varied from very weak to very strong with maximum density differences ranging from virtually zero to 0.3 percent, which, when dealing with thermally induced reservoir density stratification, is quite large.

Results

70. A computer code incorporating the stratified-flow-distribution algorithm was run with the data collected for each test, thereby producing a prediction of the individual port flows. These predictions were compared to

the observed port flows from the physical model test. A sample plot from one of the tests is given in Figure 13. The impacts of density are reflected by

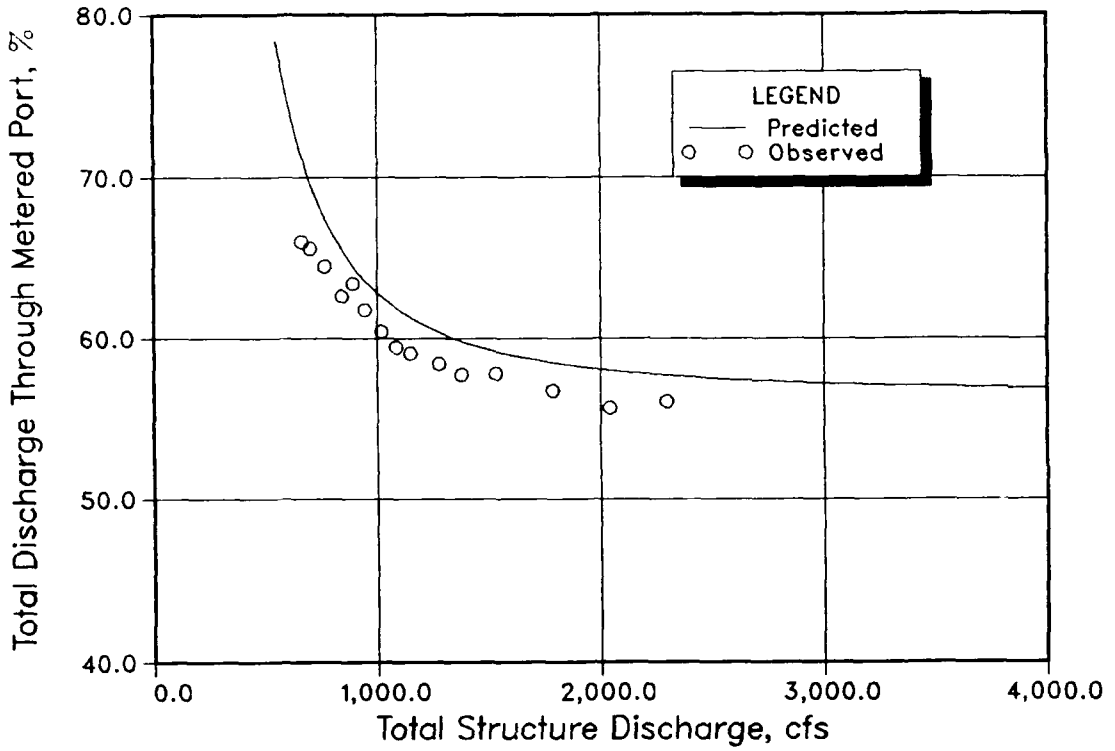

Figure 13. Sample predicted and observed port flows

the deviation of the data from horizontal in the figure. It can be seen that the density impacts were greatest at low discharges. This was true for all tests because the buoyancy head was virtually independent of flow rate. However, the other terms in the equations governing flow distribution, the head loss terms, increased greatly with discharge. Therefore, the density impact term, although still present in the equations at the higher flows, was overshadowed by the other terms, resulting in a flow distribution that approached that of the unstratified condition.

71. By the same reasoning, the density impact was most significant at very low discharges and caused buoyancy blockage. The trend toward this condition was evident in many of the resulting plots from this phase of the study. The curves became highly vertical, either upward or downward, indicating a total structure discharge near critical discharge. Critical discharge would be represented in the figure by the total discharge value at which the curve reached either 0 or 100 percent flow through the metered port. In Figure 13, the flow through the metered port was rapidly approaching

100 percent at a total prototype discharge of about 400 cfs. Therefore, all discharges below 400 cfs would also result in blockage for this stratification and port combination. Observed port flow measurements for the density blockage situation were not obtainable during these tests as the velocities were not measurable in this range.

72. Figure 14 displays the results of the stratified flow testing. Deviations between predictions and observations were generally small.

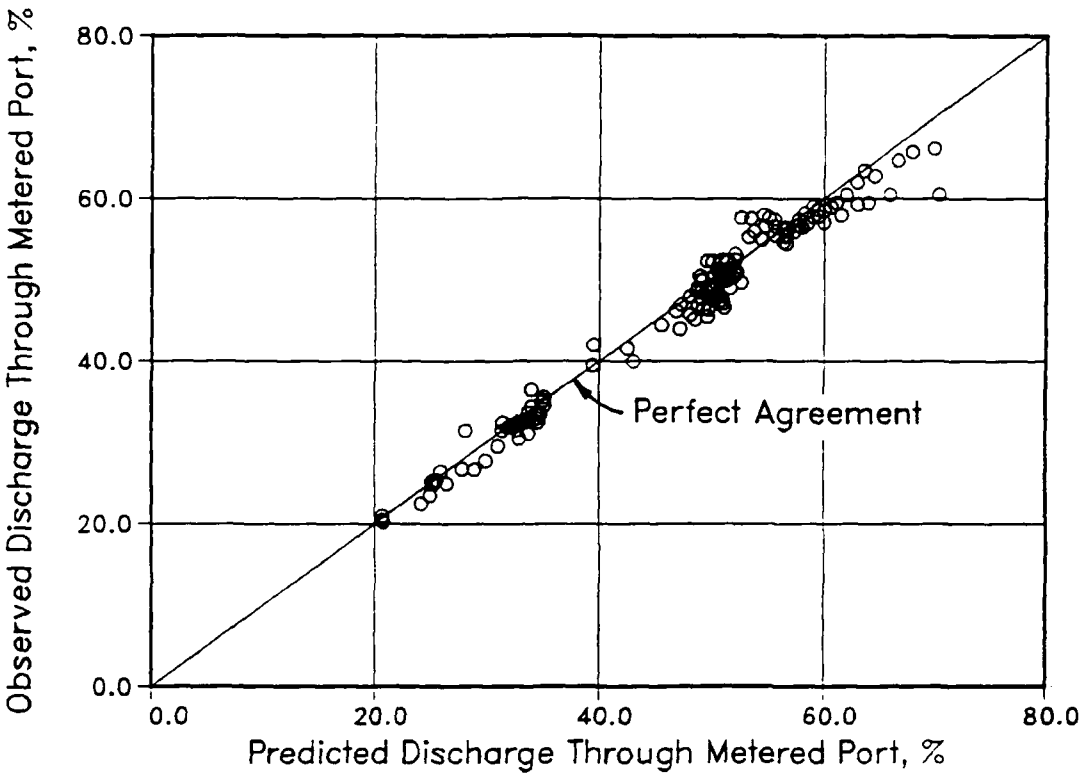

Figure 14. Predicted versus observed flow percentages

The general agreement between the predicted and observed flows was very good. Only in one case was the discrepancy greater than 10 percent. Some tests produced a uniform error over the entire range of flows, as seen in Figure 13. This type of error may be attributed to a flow measurement problem rather than to an inadequate description of the blending process as the latter would probably not have represented the shape of the observed data as well.

Summary

73. Testing with the Lost Creek physical model produced descriptions of the selective withdrawal and blending characteristics of the structure and its near-field topography. Selective withdrawal testing results demonstrated

credibility and consistency, leading to a description that permitted the prediction of the release temperature from individual port flow rates and vertical in-lake temperature profiles. Likewise, the physical model test results for blending were also credible and consistent with previous work, permitting the prediction of the individual port flows from the set of port openings, the in-lake temperature profile, and the total discharge. The close agreement in Figure 14 attested to the accuracy of the blending description. The combination of the two descriptions produced an algorithm for accurately predicting release temperatures. When the algorithm is applied to the prototype, a higher order of accuracy might be attained by minor refinement of the head loss coefficients in the blending description. This would account for any small differences between the model description and the prototype.

PART IV: LONG-TERM OPERATIONAL STRATEGY OPTIMIZATION

74. A final major aim of this study was to evaluate the long-term operational strategies of the Lost Creek intake structure. The results of the work presented to this point are directly useful in developing good daily operational guidance, but do not demonstrate any potential for long-term improvement in operations. Evaluation of seasonal operational strategies and their related tradeoffs for meeting downstream water temperature requirements was performed for the Lost Creek Lake using the OSPACE (objective space) computer code (Fontaine, Labadie, and Loftis 1982). This is an objective-space dynamic programming (DP) tool for determining the theoretically optimum reservoir operational strategy by maximizing or minimizing a predetermined, usually limited, release or in-reservoir quality characteristic. In the case of Lost Creek, this optimum operational strategy would minimize the unacceptable deviations between the release water temperature and the established downstream water temperature targets while assigning the relative priorities to different periods in the year.

75. Optimization was needed to provide foresight into the long-range consequences of immediate operational decisions regarding the reservoir's thermal resources. This would permit the selection of a port combination on a particular day that, although perhaps not providing the closest agreement between the release temperature and the target for that day, would contribute to thermal resource conservation that would prevent or decrease deviations from the release target at a later, perhaps more important, time. Objective--space DP is actually a generic tool that is useful in a variety of applications (Fontaine, Labadie, and Loftis 1982). In the OSPACE code, this tool has been coupled with the WESTEX one-dimensional reservoir model (Holland 1982) to focus on reservoir operational strategy optimization.

OSPACE Background

76. The OSPACE DP tool has been developed to have practical application in temporal reallocation of reservoir thermal resources for water quality maintenance. An example reservoir release temperature target scenario is given in Figure 15a. The symbols represent actual best-daily release temperatures and the curve, the objectives. Best-daily operations are those selected

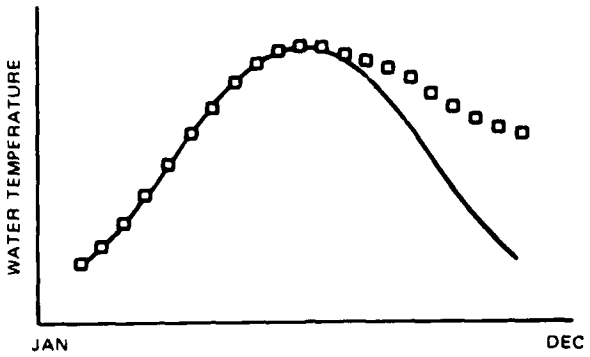

a. Best-daily operations

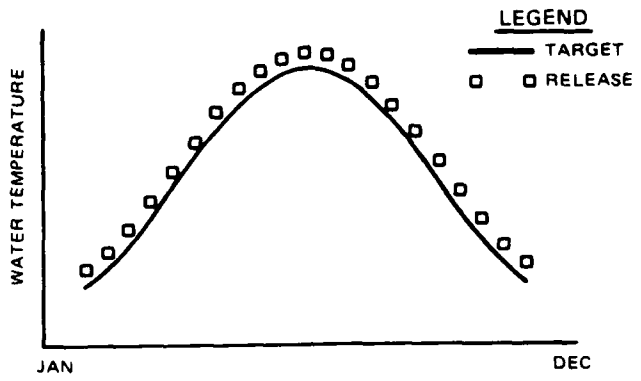

b. Optimized operations

Figure 15. Example reservoir temperature targets and releases

based upon meeting the release temperature target for that day. The targets were met through the spring and summer but were missed badly in the fall. This is a common problem in coolwater-limited reservoirs. The target temperatures are either not accessible with the release system or are often not available within the pool. Effective reallocation of the coolwater resources produced the scenario in Figure 15b. In this figure, it is obvious that the spring and summer target temperatures were intentionally missed slightly. However, this resulted in ample coolwater conservation to greatly reduce the extreme discrepancies between the release temperatures and the target temperatures in the fall, perhaps benefiting the downstream environment. If the lack of spring and summer target maintenance is acceptable, and/or the need for cooler fall releases great, these may be acceptable deviations from the original release targets.

77. The OSPACE program is capable of identifying improved operational

strategies such as the one in Figure 15b by discretizing the desired simulation period (a year or stratification season for example) into shorter intervals called stages. It then systematically and incrementally modifies the release temperature targets for the individual stages. If this modification is large enough, the intake structure port combination selected may differ from that selected to meet the original target temperature. This alternate operation will impact the reservoir's thermal composition in some manner such as conserving cool water as in this study. All target modifications are positive (targets increased) for coolwater-resource-limited problems. The model evaluates the "worth" of the different alternatives through an objective function. This is a problem-specific index that is related to the deviation between the release parameter (herein water temperature) and the original release target for that parameter. A commonly used objective function has been a sum of squared deviations. The set of operational alternatives with the lowest objective function value for the entire simulation period would represent the best scheme for meeting the established criteria over the entire period (but perhaps not for a given day).

78. The schematic in Figure 16, taken from Wilhelms and Schneider (1986), presents an easy way of understanding the processes involved. This is a simplified and abbreviated example involving only a few stages and one possible increment of deviation from a given objective at each stage (1° C). Each longitudinal segment represents a stage. There were four stages in the example. For this example, two paths were available from each initial state to the final states within each stage. States are represented in the figure by the vertical series of nodes on the left and right of each stage. For

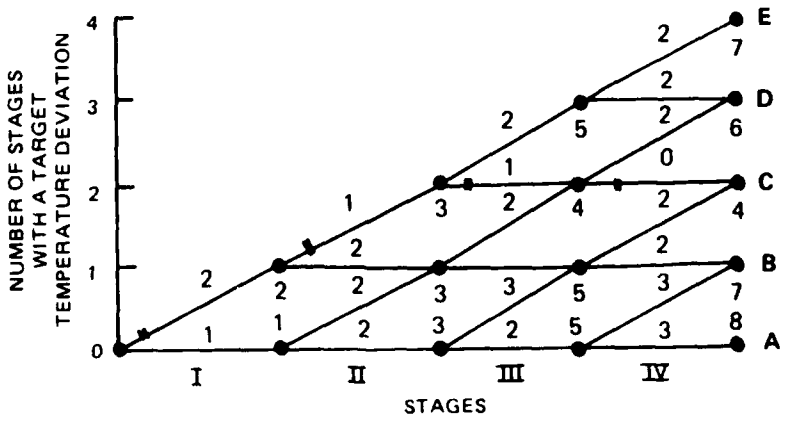

Figure 16. Abbreviated example of optimization process (from Wilhelms and Schneider 1986)

stage I, there was one initial state and two final states. A state represents the reservoir's vertical temperature profile resulting from intake structure operations attempting to meet either the original target (no deviation) or the modified target (original target plus 1° C deviation). The final states for one stage became the initial feasible states for the next stage. The two available decision paths from one stage to the next were (a) no deviation to the target, which is represented by the horizontal path line from each initial state, and (b) a uniform deviation from the original target temperatures within that stage of some value, in this case a 1° C increase, which is represented by the sloped path line from each initial state. The values located immediately above every path line, although contrived just for this example, represented the objective function value associated with that particular path for that stage. The values below each node point represented the minimum cumulative values to that point indicating the least-cost path, in terms of objective function, to that state.

79. The ending state A, in the figure, for the simulation period would correspond to an operational policy that took no deviation from the original targets over the entire period (best-daily operational approach). The ending state B would correspond to a modification from the original target in one of the four stages and no modifications in the other three. The objective function values associated with the individual modification of the targets in the four stages would determine which single stage would be selected. The ending state C would represent modification in two of the four stages; D, three of four stages; and E, uniform modification over the entire simulation period.

80. Each of the ending states (A through E) had an associated cumulative objective function value located below the ending nodes in the figure. The ending state with the smallest objective function value, based on the criteria established in the formulation of the objective function, represented the best operational strategy to adopt for the simulation period. In the figure, ending state C had the lowest objective function value at 4. The double tick marks indicate the optimum path associated with this ending state. In this example, the optimum release temperature strategy consisted of a deviation in the first two stages and no deviation in the last two stages.

81. Each state (including the ending states) contained a least-cost path back to the origin that represents the first day of optimization. The optimum strategy was determined by beginning a backward tracing at ending

state C that followed each segment of the least-cost path determined en route to the optimum state. These segments included no deviations for stages III and IV, as indicated by the double ticks on the horizontal lines. The double ticks on the sloped lines for stages I and II reflect the deviations.

WESTEX Verification and Final Verification

82. Before OSPACE could be applied to Lost Creek, coefficient development was required. The WESTEX-compatible data sets employed by the OSPACE code must include certain site-specific coefficients regarding thermal energy influx distribution and internal mixing characteristics. The WESTEX model without the outer DP shell was used in the development of the coefficients. The first action taken was data collection. Portland District provided 2 years of hydrologic and meteorologic data (1978 and 1979) in WESTEX-compatible format. Historical port operations for these years were also provided by the Portland District. Observed in-lake temperature profiles and approximate water-surface elevations were taken from two Portland District documents (USAED, Portland, 1979, 1980). The input files were modified to include the selective withdrawal description and head loss coefficients developed earlier in this study. A check of the water budget was performed for both years. The initial depth was specified and the model was run. The water surface matched the observed values closely, indicating an appropriate balance of inflows and outflows in the hydrologic description.

83. An evaluation of the heat exchange and distribution coefficients was then possible. Those coefficients governing vertical distribution of thermal energy influx were β , which represents the fraction of the total incoming solar energy absorbed in the top 2 ft of the pool, and λ , which is a coefficient of extinction to distribute exponentially the remaining solar energy vertically. The range of β is from 0.0 to 1.0 while the normal range of λ is from 0.0 to about 3.0 per foot.

84. The mixing process in the model normally permits the adjustment of a mixing coefficient and an entrainment coefficient. Based upon concurrent work on Lost Creek by Davis and Schneider,* an alternative formulation for

* Unpublished data, 1988, J. E. Davis and M. L. Schneider, US Army Engineer Waterways Experiment Station, Vicksburg, MS.

mixing was adopted. This formulation contained the original WESTEX mixing coefficient multiplied by an exponential expression containing the density gradient at the vertical point in question and a second coefficient. This formulation was developed such that in a homogeneous region, the exponential portion would reduce to unity, yielding the original mixing coefficient. The mixing formulation regulates the amount of diffusive mixing permitted between model layers and can range from 0.0 to infinity. The entrainment coefficient controls the amount of surface water mixed with the inflows. Entrainment effectively modifies the inflow temperature and density, causing the inflow to seek a different elevation within the pool as compared to no entrainment. The normal range for this coefficient is 0.0 to 1.0 with the previous default set at 0.0.

85. Several model simulations were made in "verification" mode with the 1979 data set, which was arbitrarily chosen for model coefficient adjustment. Verification mode meant that the port selection subroutines within the WESTEX model were not accessed, but port operations were made as they were historically in the year simulated. Several combinations of the four coefficients were attempted. The results from the comparisons between model predictions and observed data were evaluated statistically using the reliability index described in Appendix B. The combination of coefficients that produced the best correlation between the prototype and model-predicted data was β of 0.40, λ of 0.2 per foot, mixing coefficients of 20 and 0.5×10^{10}, and an entrainment coefficient of 0.3. Figure 17 shows the model predictions. Comparisons are shown for 7 days corresponding to 1 day of each month from March through October (except June) of 1979. These are identifiable by the Julian day on each plot. Julian day refers to the sequential day in the calendar year with 1 January being first. The reliability index (RI) of the chosen grouping of coefficients was 1.14. Perfect correlation would constitute an index of 1.0.

86. Once the best fit of the 1979 data had been achieved, the coefficients were installed in the 1978 data set and final verification of the model was performed. The results are given in Figure 18 with the same notations as in the previous figure. The correlation was very good with a reliability index of 1.13, which was better than the initial verification phase results.

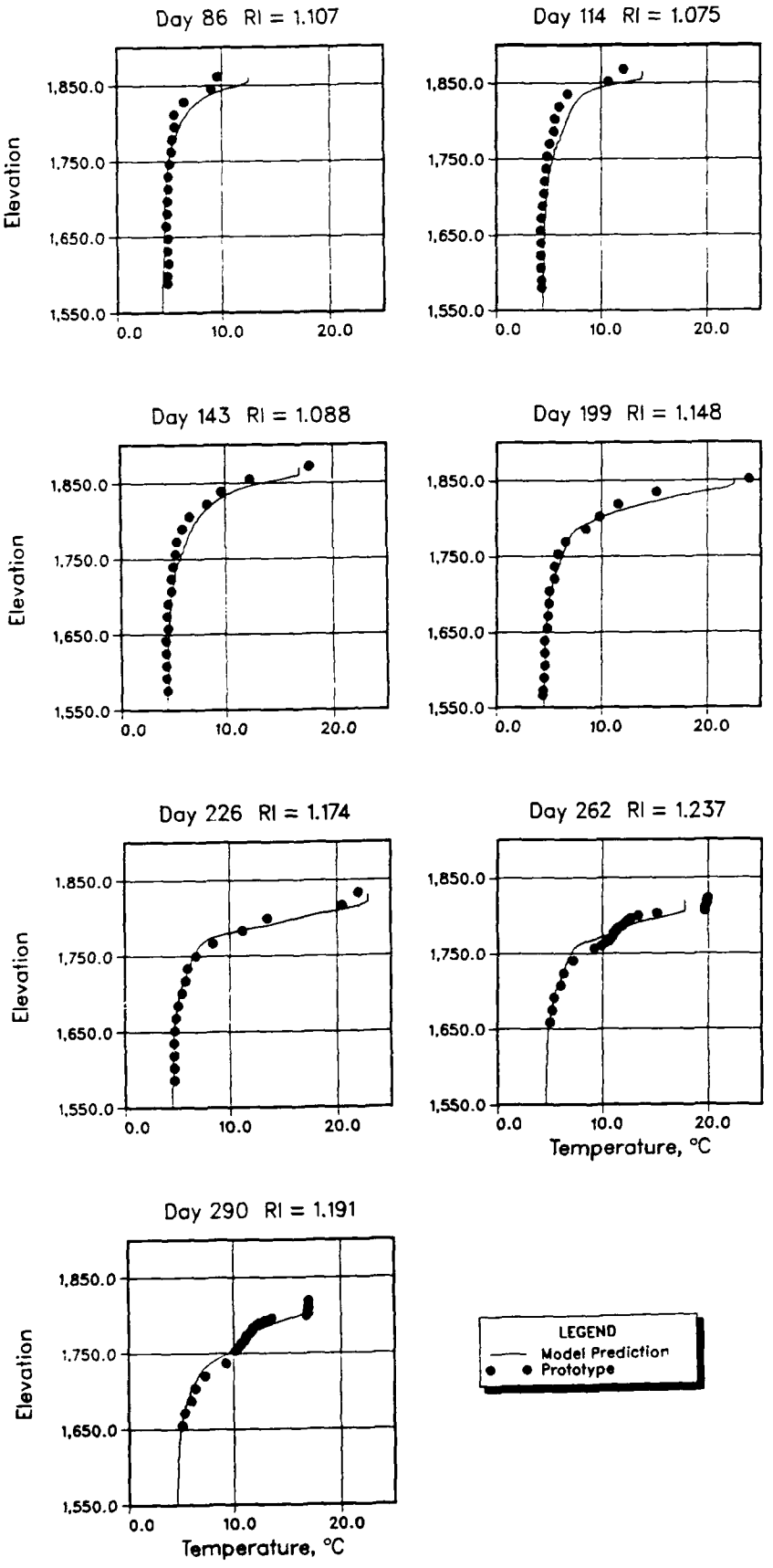

Figure 17. WESTEX verification of 1979 data

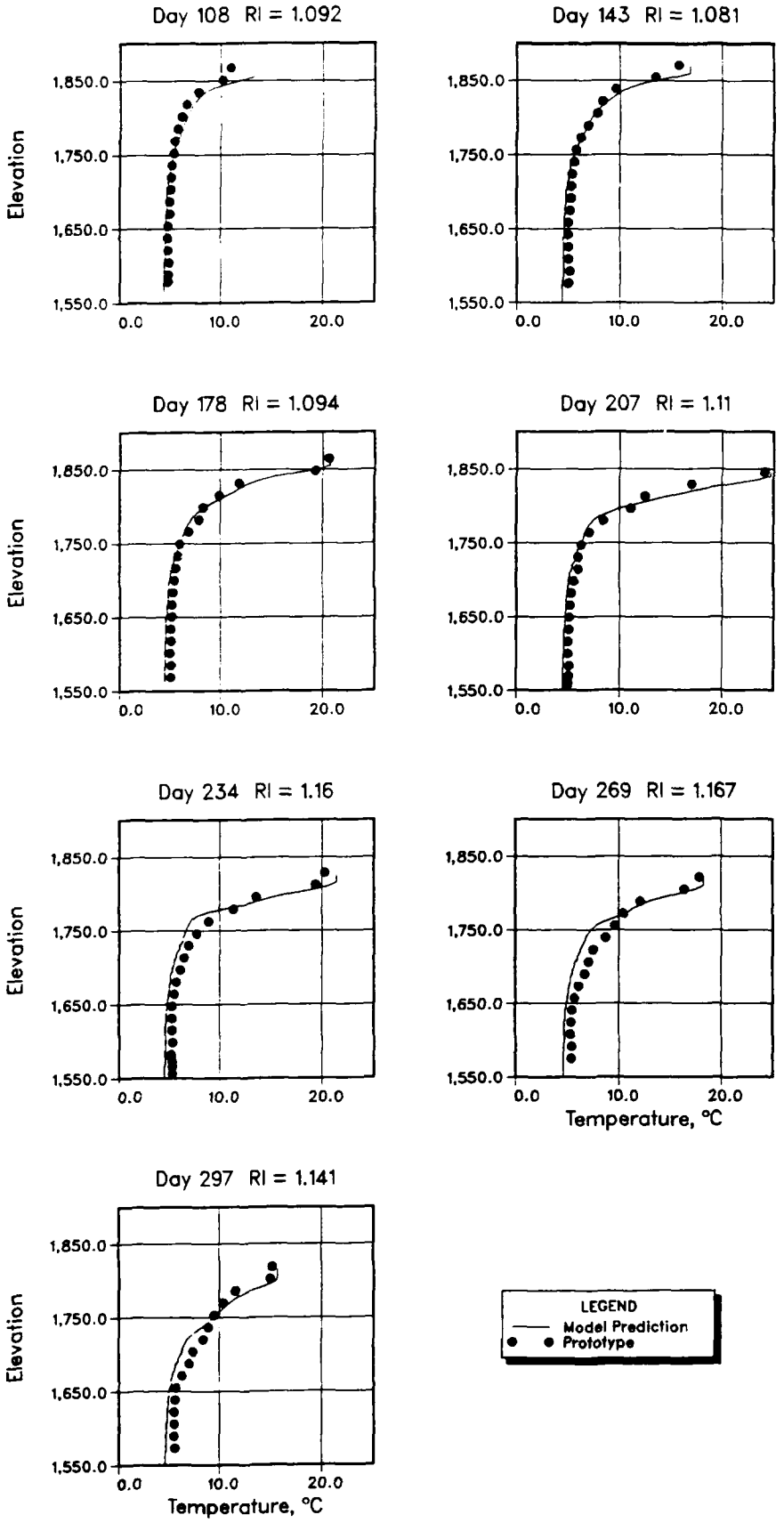

Figure 18. WESTEX verification of 1978 data

Application of OSPACE to Lost Creek

87. Several preliminary steps were necessary in the application of the OSPACE model to Lost Creek. These included model modification, input data gathering, and objective function development. The mode of model operation had to be changed to prediction from verification for the optimization work. Before that was possible, extensive code modifications were necessary. In prediction mode, the WESTEX model selects port operations based upon the desired release water temperature target, the pool water-surface elevation, and the discharge. The model was not yet capable of making this selection in a single-wet-well blending mode such as that at Lost Creek. This section of code was rewritten specifically for the Lost Creek study. The blending algorithm was added to the WESTEX model to predict the best possible port combination for the given criteria. These coding changes included some operational criteria established by Portland District, which stated that one intake port would be opened for each 1,000-cfs increment of discharge, or fraction thereof, and that at least 15 ft of submergence on port center-line elevations was necessary for port operation.* Also, for flows less than 1,000 cfs, one or two intake ports might be opened, whichever provided the release temperature closest to the target temperature. No minimum port flows were established and zero flow was adopted as a minimum.

88. Initial blending work, discussed in the previous sections, had been based on the assumption that the density and temperature of the flow entering an intake port were essentially equal to the port center-line elevation values of those constituents in the reservoir profiles. After some testing of the code, this assumption was modified. Occasionally, the error induced by this assumption was large enough to cause an errant port selection. An additional call to the selective withdrawal portion of the code was added, making the assumption of individual port withdrawal constituent values unnecessary. This modified version of WESTEX, which was capable of predicting the best port combination to meet daily release water temperature targets within the established criteria, was then incorporated into the OSPACE model.

---

* Personal communication, 28 August 1986, with Mr. R. A. Cassidy, Environmental Engineer, US Army Engineer District, Portland, Portland, OR.

Input data

89. A WESTEX-format data file along with a short file containing DP inputs were needed for the OSPACE model. The years to be used were limited to 1978 and 1979, which at the time were the only years for which data sets had been developed for Lost Creek. The 1978 and 1979 data were reformatted into prediction mode data sets. These formats required the specification of release target temperatures. An updated release target temperature scenario, agreed upon by Portland District and the Oregon Department of Fish and Wildlife early in 1987,* was forwarded to WES by Portland District for use in these evaluations.

90. To further define the temperature objectives, Portland District provided priorities and release temperature deviation tolerances for different periods during the year. These ranged in priority from 1 to 3 and in tolerance from 0.5° C to 2.0° C. The result was a division of the year into five periods according to tolerance and priority. As can easily be seen by the priorities (1 being most important) and the tolerances in Table 1, the late summer, fall, and winter were the more important times for the downstream temperature to match the target temperatures for the fishery.

Objective function

91. Development of an objective function was also necessary. Two separate objective functions were developed to reflect the importance of meeting the release target temperature for a particular stage based upon the priorities and tolerances established in Table 1. A summed squared deviation between the release water temperature and the original target temperature was employed as a base means of comparing alternatives. An additional penalty was then added for missing the target temperature by more than the allowable tolerance. The first index employed a linear function of the priority multiplied by the temperature deviation in excess of the established tolerance. The second objective function was similar except that the priority function was logarithmic. This was done to amplify the influence of the priority system. These approaches produced the objective function formulations in Equations 8 and 9:

---

* Personal communication, 17 March 1987, with Mr. R. A. Cassidy, Environmental Engineer, US Army Engineer District, Portland, Portland, OR.

Table 1

Lost Creek Lake Release Temperature Schedule

Date	Priority	Tolerance °C	Target Temperature °C
01 Jan	1	2.0	3.0
07 Jan	↓	↓	↓
14 Jan			
01 Feb			
07 Feb			
14 Feb			
21 Feb			
01 Mar	3	2.0	4.7
07 Mar	↓	↓	4.9
14 Mar			5.3
21 Mar			5.5
01 Apr			5.8
07 Apr			6.3
14 Apr			6.9
21 Apr			7.6
01 May			8.2
07 May			8.5
14 May	2	1.0	8.5
21 May	↓	↓	9.0
01 Jun			↓
07 Jun			
14 Jun			
21 Jun			
01 Jul			
07 Jul			
14 Jul			11.1
21 Jul			11.1
01 Aug			12.8
07 Aug			12.8
14 Aug			12.8
21 Aug	1	0.5	12.8
01 Sep	↓	↓	11.6
07 Sep			10.9
14 Sep			6.7
21 Sep			6.0
01 Oct			5.2
07 Oct			4.5

(Continued

Table 1 (Concluded)

Date	Priority	Tolerance °C	Target Temperature °C
14 Oct	1	1.0	4.0
21 Oct	↓	↓	3.0
01 Nov			↓
07 Nov			
14 Nov			
21 Nov			
01 Dec			
14 Dec			
21 Dec			

$$\text{OBJECTIVE FUNCTION} = (T_r - T_t)^2 + (|T_r - T_t| - TOL) \times (4 - PRI) \quad (8)$$

$$\text{OBJECTIVE FUNCTION} = (T_r - T_t)^2 + (|T_r - T_t| - TOL) \times 10^{(4 - PRI)} \quad (9)$$

where

T_r = predicted release water temperature for that day, °C

T_t = targeted release water temperature for that day, °C

TOL = deviation tolerance established for that day, °C

PRI = priority established for that day

92. The part of each of these formulations containing the priority information was added only when the difference between the release temperature and the target temperature exceeded the tolerance. The objective function in Equation 9 imposed a very severe penalty for missing the target temperature in excess of the tolerance during a priority 1 stage to provide the impetus for potential modifications during the less critical periods associated with priorities 2 and 3. The model was further modified at this point to compute objective function values on a daily basis rather than once per stage. The potential daily operational changes at Lost Creek required that the objective function be sensitive to daily deviations between targets and releases.

Results

93. Initial results from optimization simulations for both study years indicated essentially no potential for improvement in the first 11 weeks of the calendar year as the reservoir was only very slightly stratified. Since the OSPACE program may make several hundred calls to the WESTEX subroutines,

the judicious elimination of the first 77 days from simulation greatly reduced computation time and costs.

94. Several model parameters were selected during preliminary simulations. These included the number of stages (40), the number of days per stage (7), the initial day of optimization (78), and the final day of optimization (357). Fewer days in each stage would have increased the resolution of the results but would also have increased the number of stages and the computational requirements. The number of days per stage was established at seven since this was considered the minimum number feasible to keep the number of stages required at a reasonable level. The initial day of optimization was selected because of its correspondence with the development of significant temperature stratification and the beginning of a 7-day period on the Julian calendar. The ending day was selected for similar reasons. It was determined that most of the thermal stratification had subsided for the winter by this time and this date coincided with the end of a 7-day period.

95. Also selected during preliminary tests was the number of allowable ending states for each initial state (4). This selection permitted the incremental modification of the target temperature as opposed to two ending states, which would permit only modification or no modification. Four rather than five ending states were selected to maintain reasonable computational costs. Within each stage, the model was allowed to select among four alternatives: no modification to the original target temperatures, a +1.4° C (square root of 2) uniform modification, a +2.0° C (square root of 4) uniform modification, or a +2.45° C (square root of 6) uniform modification. The maximum deviation was chosen to exceed the maximum allowable temperature deviation tolerance already established. Each of these ending states was permitted for each initial state within each stage. This resulted in a maximum summed squared modification for the entire simulation period of 240° C squared. Therefore, the 121 possible ending states for the entire simulation period ranged from 0 to 240° C squared in increments of 2.

Linear objective function equation results

96. Output from the OSPACE model is essentially a set of modified target temperatures that induces operations producing the smallest objective function value over the entire simulation period. If the objective function equation has been properly selected, these modifications to the target

temperatures provide long-term improvement in the structure's operational strategy. The model-proposed revisions in target temperatures stemming from simulations with the linear objective function (Equation 8) are given in Table 2. The objective function values for the best-daily operations were 1,948.0° C squared for 1978 and 1,704.0° C squared for 1979. Optimization produced objective function values of 1,546.0 and 1,561.0, respectively. The proposed modifications during the priority 1 periods induced little change in the release temperature. Because the releases during these periods were already too warm, warming the target did not produce a substantial impact. Often, this effect was limited to a change from one port to the next higher port within the hypolimnion. This type of change in structure operation produced very little change in release temperature, but caused a measurable amount of resource conservation by withdrawing water from higher in the pool than before.

97. Results of optimization testing with the linear objective function revealed at least a small opportunity for improvement of current operations. The plots of optimized and nonoptimized (best-daily) operation release temperature deviations from the original release target temperatures are provided in Figure 19. The best-daily operation data were calculated using the model-predicted release temperatures for best-daily operations minus the original target temperatures. The optimized operation data were calculated using the model-predicted release temperatures for optimized operations (using the linear objective function equation) minus the original target temperatures. These deviations from the original targets were virtually always positive, indicating that the release temperatures were too warm. Between Julian days 60 and 260, the solid line deviated only slightly from zero, demonstrating good capabilities in meeting the targets. However, the resource limitation problems that prompted this study surfaced after day 260 with deviations for daily operations reaching almost 6° C in 1978 during the highest priority period for the fishery. At this point, the coolwater resource within the reservoir had been depleted.

98. Optimized operations promoted larger deviations during the spring and summer periods to achieve an amount of cooling of the releases in the fall (after day 260). For 1978, this cooling was short-lived, lasting only until about day 310 when the temperatures of the optimized releases and the daily releases converged. For 1979, however, the improvement was small but was

Table 2

1978 Model-Proposed Target Temperature Modifications

Using the Linear Objective Function

Date	Stage No.	Priority	Tolerance °C	Modification °C
	Modifications from 1978 Simulation			
Mar 19-25	1	3	2.0	+2.5
Mar 26-01	2	3	2.0	+2.5
Apr 02-08	3	3	2.0	+2.5
Apr 09-15	4	3	2.0	+2.5
Jun 04-10	12	2	1.0	+2.5
Jun 11-17	13			+2.5
Jun 25-01	15			+1.4
Jul 02-08	16			+1.4
Jul 09-15	17			+1.4
Jul 16-22	18			+1.4
Jul 30-05	20			+2.0
Aug 06-12	21			+2.5
Aug 13-19	22			+2.5
Sep 24-30	28	1	0.5	+1.4
Oct 01-07	29	1	0.5	+2.5
Oct 08-14	30	1	0.5	+2.5
	Modifications from 1979 Simulation			
Apr 09-15	4	3	2.0	+1.4
Apr 16-22	5	3	2.0	+2.0
Apr 23-29	6	3	2.0	+1.4
Apr 30-06	7	3	2.0	+1.4
May 07-13	8	3	2.0	+2.5
May 21-27	10	2	1.0	+2.5
May 28-03	11			+2.5
Jun 04-10	12			+2.5
Jun 11-17	13			+1.4
Jun 18-24	14			+1.4
Jun 25-01	15			+2.5
Jul 02-08	16			+2.5
Jul 08-15	17			+2.5
Jul 16-22	18			+2.5
Jul 30-05	20			+1.4
Aug 06-12	21			+2.5
Aug 27-02	24	1	0.5	+1.4
Sep 03-09	25	1	0.5	+2.5
Sep 24-30	28	1	0.5	+2.5
Oct 08-14	30	1	0.5	+2.0

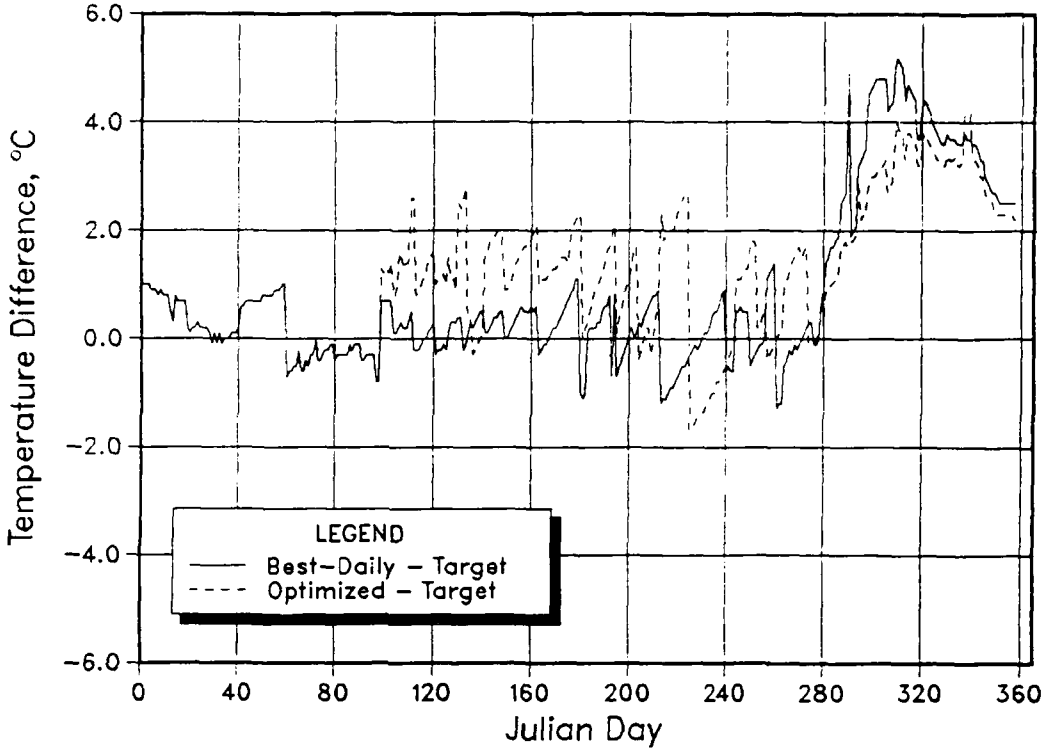

a. 1978

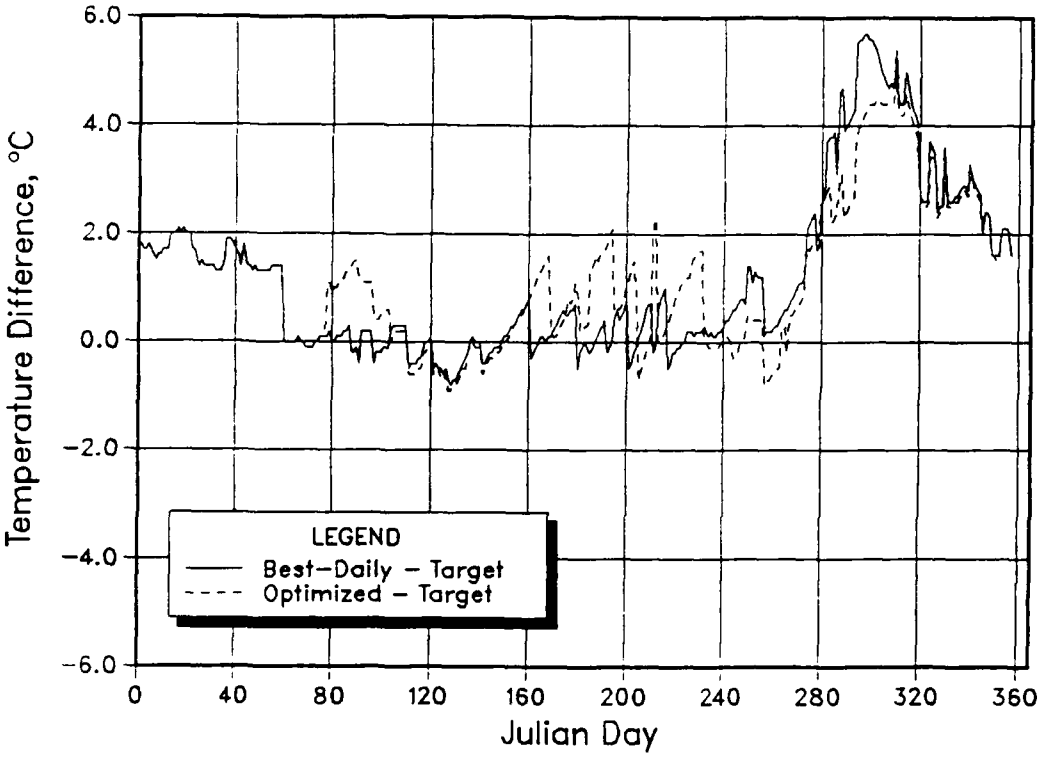

b. 1979

Figure 19. Deviations of optimized operations and best-daily operations from original targets using the linear objective function equation

noticeable (greater than 0.3° C) even at day 357, the end of simulation. For both years, the amount of improvement in the fall was less than the requested spring and summer deviations from the targets, demonstrating the influence of the priority system. The magnitude of the summed squared deviations during the spring and summer was greater than the reduction in summed squared deviations for the fall. Therefore, in the absence of a priority system, these deviations would not have been advised.

99. A variation of Figure 19 is given in Figure 20. This figure shows the release temperatures for optimized operations minus the release temperatures for best-daily operations. These graphs reveal the overall impact of optimizing operations on the downstream environment. The days that have a positive difference reflect periods of coolwater resource conservation with optimized operations. The negative values show the cooling of the release temperatures compared to best-daily operations as a result of the conservation effort. However, careful examination of this figure shows that optimized operations would result in an overall warming of the releases since the sum of the positive differences was greater than the sum of the negative differences.

100. Figure 20 also provides some quantification of the sacrifices (temperature increases) and the potential improvements (temperature decreases) in meeting release temperatures. For 1978, most of the improvements were 1° C or less. The exception occurred between days 280 and 300 when the improvements averaged about 1.5° C. Only occasionally did optimization cause increases in spring and summer release temperatures that exceeded 2° C. For this year, no modifications were possible between days 104 and 160 as daily operations already caused port selections as high as possible in the pool. Therefore, an increase in the release temperature was not requested. For 1979, a similar situation occurred between days 78 and 98. For this year, the increase in release temperatures approached 3° C for a 2-week period in late summer. During the remainder of the spring and summer, the differences were usually less than 2° C. The improvement in the fall as a result of these differences in the spring and summer neared 2° C for a short time and exceeded it for one day.

101. The model-predicted release temperatures for best-daily operations and for optimized operations (using the linear objective function) are presented with the original target temperatures in Figure 21. These graphs further illustrate the good agreement between the best-daily operation release

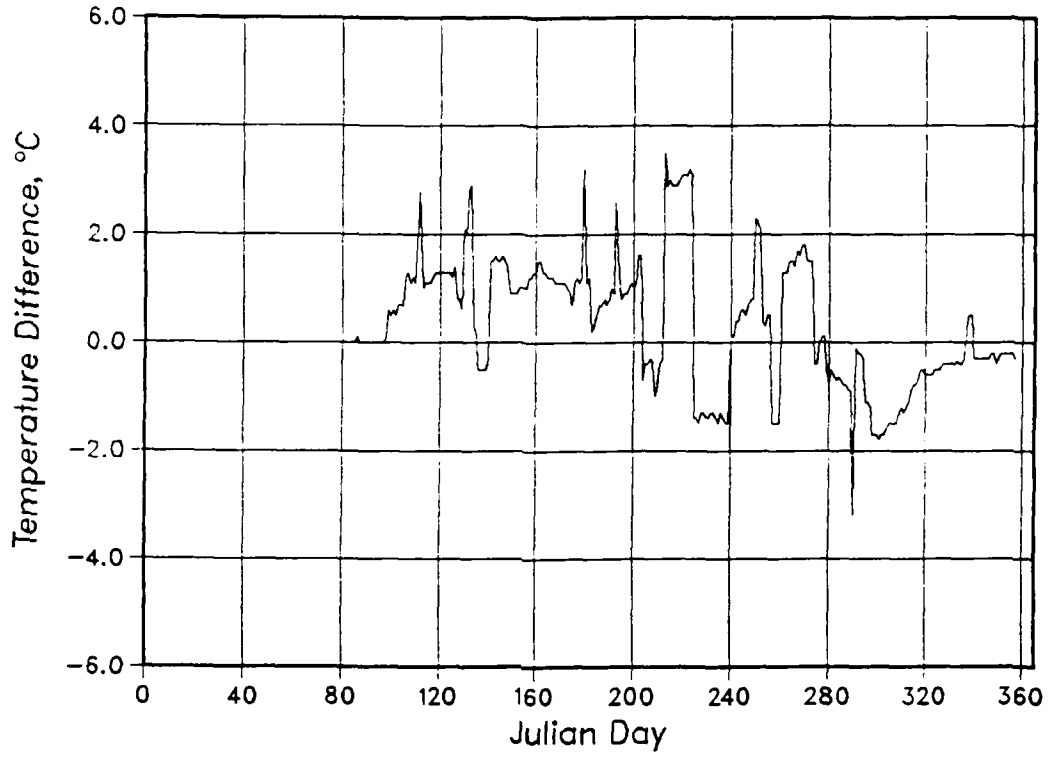

a. 1978

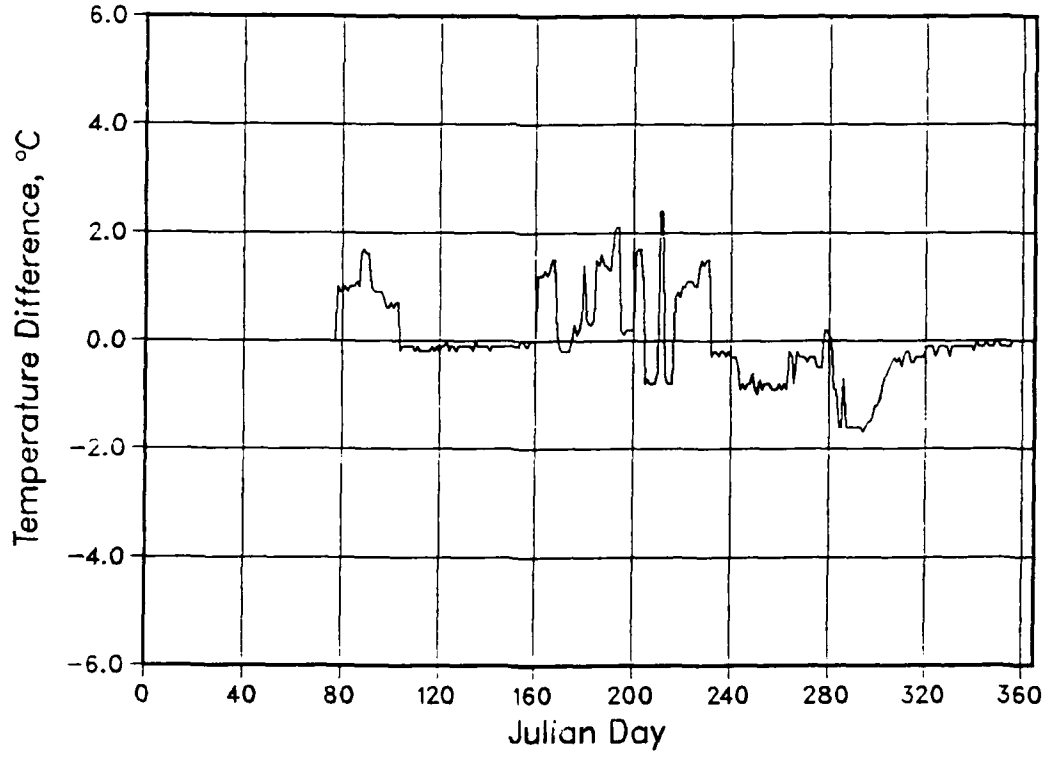

b. 1979

Figure 20. Differences between the optimized operation release temperatures and the best-daily operation release temperatures for the linear objective function

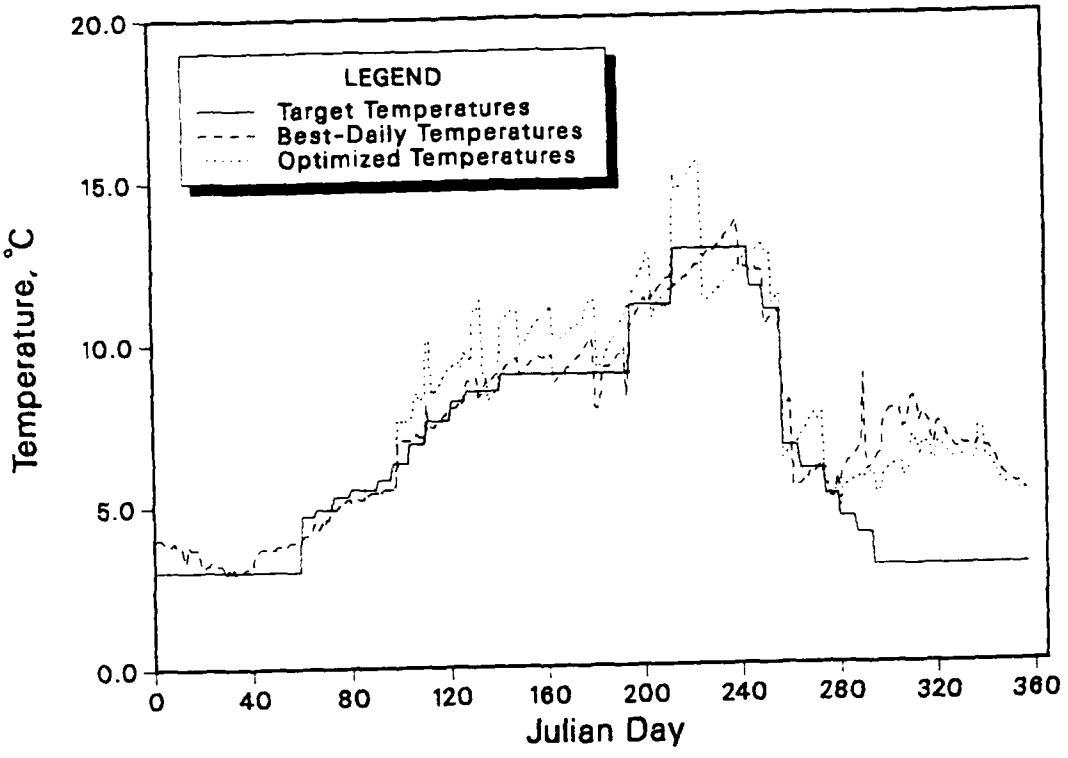

a. 1978

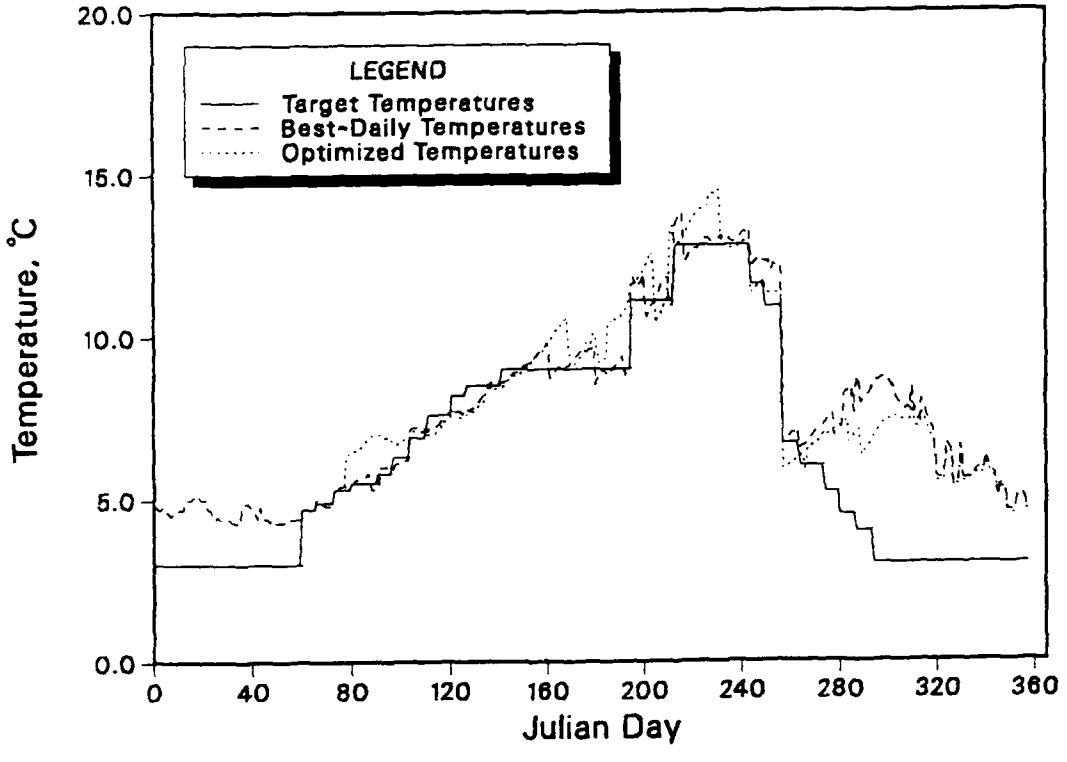

b. 1979

Figure 21. Comparison of release temperatures for linear objective optimization

temperatures and the targets between days 60 and 260, and the poor agreement between the same in the fall and winter. Also evident in these graphs is the fact that more substantial modifications were suggested for 1979 than for 1978. This was due, at least in part, to the extended period during which no modification was possible during 1978.

Logarithmic objective
function equation results

102. Simulations were also conducted with the logarithmic objective function (Equation 9) described earlier. These simulations resulted, as was anticipated, in a larger number of suggested modifications to the target temperature strategy. This was anticipated since the logarithmic objective function effectively exaggerated the priority system compared to the linear objective, making the priority 2 and priority 3 periods even less important than the priority 1 periods. The objective function values for these simulations were considerably larger than those observed with the linear objective function due to the larger penalty employed by the former. The objective function values computed for daily operations were 235,196° C squared for 1978 and 205,140° C squared for 1979. These were reduced by optimization to 152,562 and 139,893, respectively. The model-proposed modifications to the release targets for the logarithmic objective function equation are given in Table 3. The priority 1 modifications were again limited to changes in port operations within the hypolimnetic region that produced little change in release temperature while affording a small amount of conservation by avoiding the lowest ports. Not only were more stages modified using the logarithmic objective function as compared to the linear, but almost all the modifications were the maximum allowable (2.5° C) for the logarithmic evaluations.

103. Graphs similar to those in Figure 19 were created for the logarithmic objective function work and are shown in Figure 22. The solid lines are the same as those in Figure 19. For 1978, the summer (days 160 to 230) deviations from the release targets were often above 3° C and were near 4° C for several days. These were considerably larger that the deviations from the linear objective function work. However, the benefits were increased accordingly in the fall. For the linear objective function results for 1978, the deviation of the optimized releases from the targets exceeded 4° C for an extended period between days 290 and 320. However, the increased sacrifices with the logarithmic objective function values resulted in deviations that

Table 3

Model-Proposed Target Modifications Using the Logarithmic Objective Function Equation

Date	Stage No.	Priority	Tolerance °C	Modification °C
	Modifications from 1978 Simulation			
Mar 19-25	1	3	2.0	+2.5
Mar 26-01	2	3	2.0	
Apr 02-08	3	3	2.0	
Apr 09-15	4	3	2.0	
Jun 10-17	13	2	1.0	
Jun 18-24	14			
Jun 25-01	15			
Jul 02-08	16			
Jul 09-15	17			
Jul 16-22	18			
Jul 23-29	19			
Jul 30-05	20			
Aug 06-12	21			+1.4
Aug 13-19	22			+2.5
Aug 20-26	23	1	0.5	+2.5
Aug 27-02	24	1	0.5	+2.5
	Modifications from 1979 Simulation			
Apr 09-15	4	3	2.0	+2.5
Apr 16-22	5			
Apr 23-29	6			
Apr 30-06	7			
May 07-13	8			
May 14-20	9	2	1.0	
May 21-27	10			
May 28-03	11			
Jun 04-10	12			
Jun 11-17	13			
Jun 18-24	14			
Jun 25-01	15			
Jul 02-08	16			
Jul 09-15	17			
Jul 16-22	18			
Jul 23-29	19			
Jul 30-05	20			
Aug 06-12	21			
Aug 13-19	22			
Sep 03-09	25	1	0.5	
Oct 08-14	30	1	0.5	+1.4
Oct 15-21	31	1	1.0	+2.5
Oct 22-28	32	1	1.0	+1.4

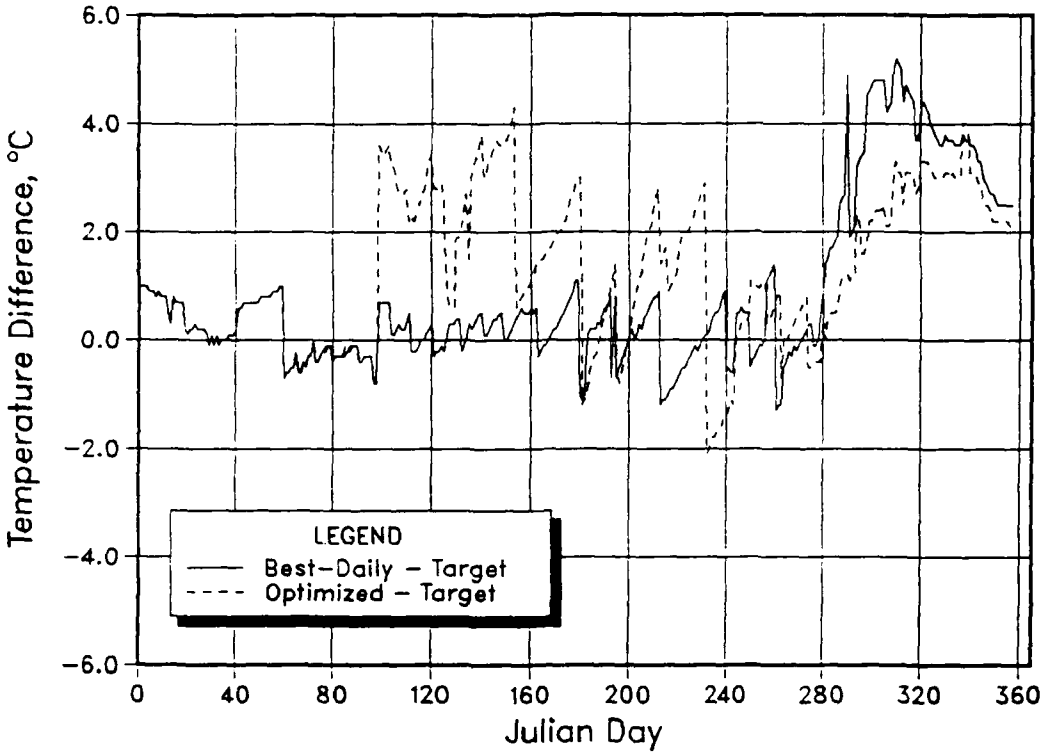

a. 1978

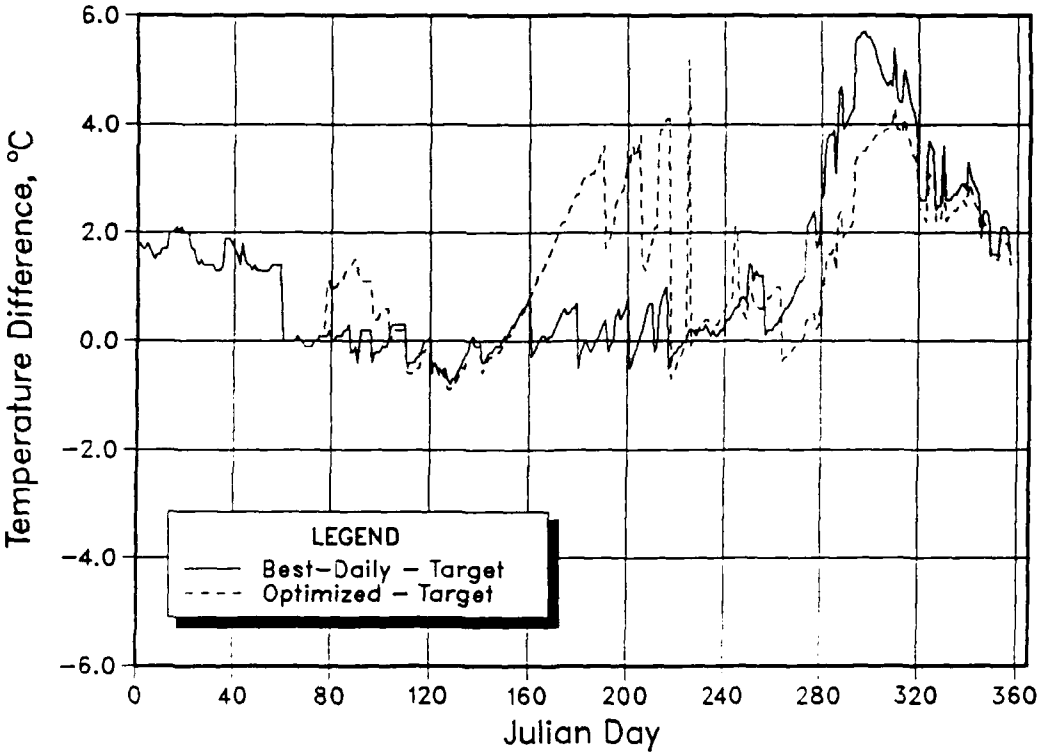

b. 1979

Figure 22. Deviations of optimized and best-daily operations from original targets using the logarithmic objective function equation

exceeded 4° C on only 2 days after day 290. Results for 1979 were equally improved with the logarithmic objective function. From Figure 19, the optimized releases in the fall yielded deviations from the targets that neared 4° C. The use of the logarithmic objective function equation produced summertime deviations of 2 to 4.5° C, but fall deviations were reduced to near 3° with the exception of a 3-day period with 4° C deviations.

104. Differences between the optimized operation releases and the daily releases can be seen in Figure 23 (comparable to Figure 20 with the linear objective function equation). These graphs clearly demonstrate the sacrifices, reflected by the positive differences, and the benefits, reflected by the negative differences in the fall. Benefits diminished toward the end of the simulation periods as the reservoir became meteorologically dominated and operations became less important. For a short period, improvements exceeded 2° C for both years. These benefits must be weighed against up to 4.5° C warming of the releases during the spring and summer. Results from the linear objective function equation evaluations were also included in these graphs to permit comparison between the alternatives.

105. Release temperatures for optimized and best-daily operations and release targets are graphed in Figure 24. Again, the costs and benefits are obvious. The largest sacrifices for 1978 were taken from June to mid-August (days 150 to 230). The sacrifices for 1979 were taken over a longer period. Large deviations were taken between early March and late June (days 90 to 180) and again between mid-July and mid-August (days 200 and 230).

106. In general, optimization produced some fall cooling of the releases that was sought, but not without some sacrifices during the spring and summer. However, the late fall and winter releases, even with optimization using the logarithmic objective function, were still considerably warmer than the release targets. Both the sacrifices and the benefits in release temperature-target correlation were larger with the logarithmic than with the linear objective function. The maximum 1-day benefits, quantified by the differences between the daily and optimized release temperatures, were 1.7 and 3.2° C with the linear objective function for 1978 and 1979, respectively. For the logarithmic objective function, the maximums were 2.3 and 3.6° C for the same years, respectively.

107. Each optimization revealed a period in the fall during which most of the benefits were realized. This period was longer for the logarithmic

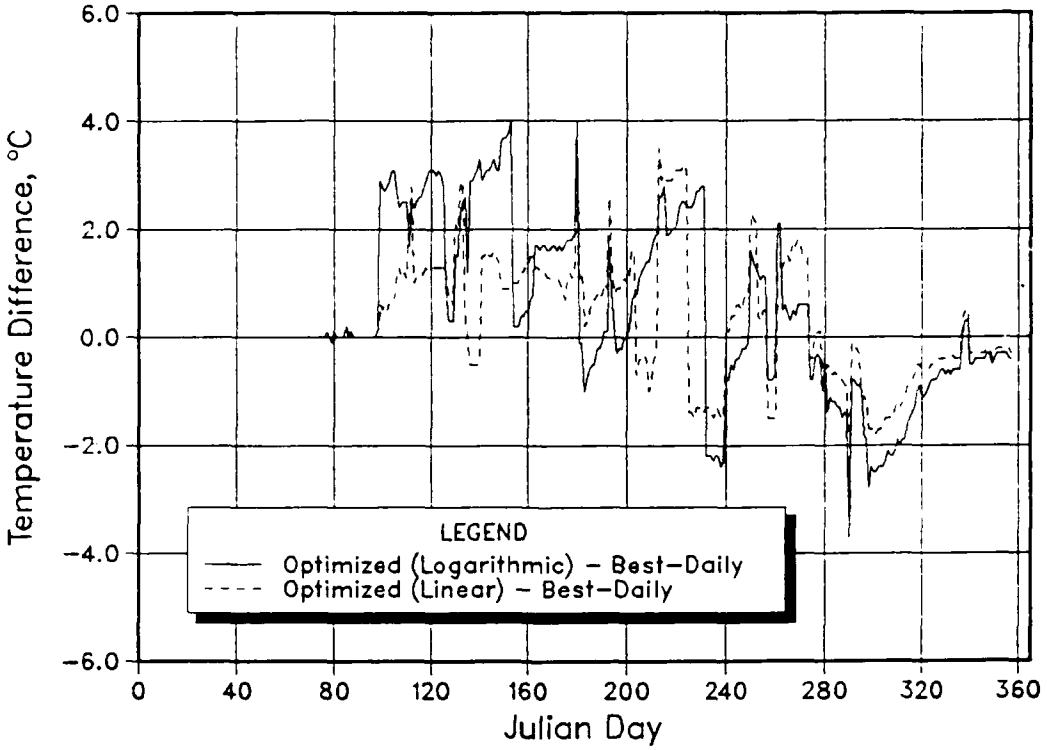

a. 1978

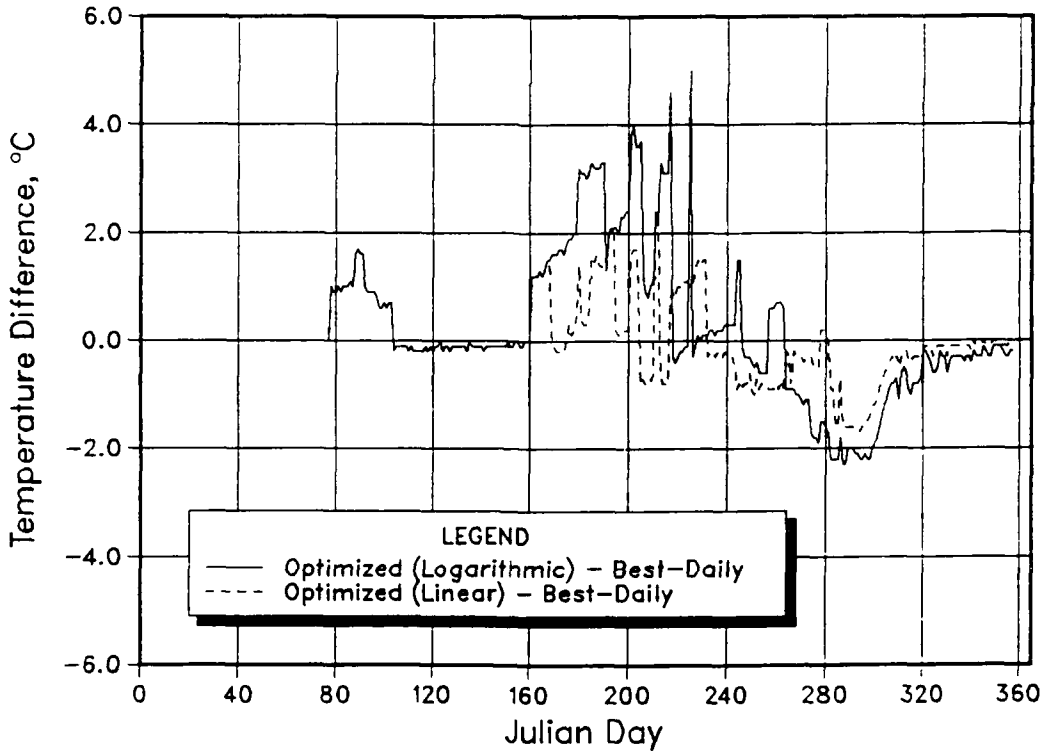

b. 1979

Figure 23. Differences between the optimized operation release temperatures and the best-daily operation release temperatures for the logarithmic objective function

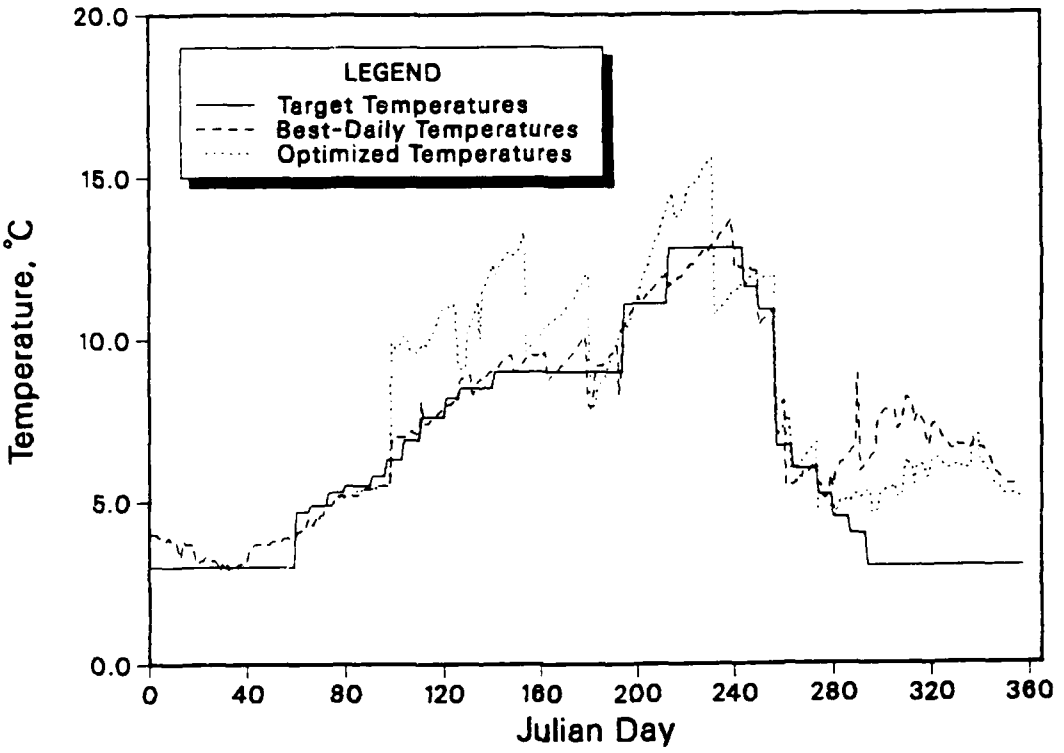

a. 1978

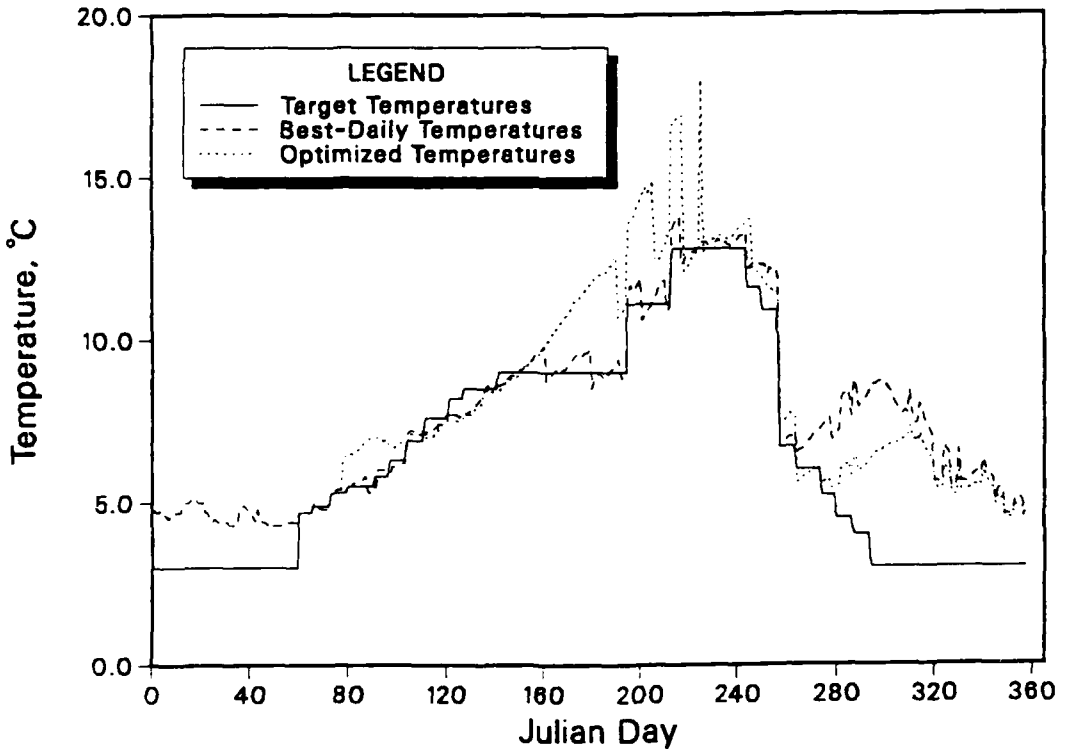

b. 1979

Figure 24. Comparison of release temperatures for logarithmic objective optimization

objective function results than for the linear objective function results. For 1978, the linear objective function results produced a 28-day continuous period, from Julian days 276 to 304 (2 October through 30 October) during which the improvement in release temperature due to optimization was at least 0.5° C. The same statistic from the logarithmic objective function work for 1978 was 56 days (20 September through 14 November). Similar comparisons were made for the 1979 simulations. The linear objective function simulations produced a 28-day continuous period of improvement of 0.5° C or larger (21 October through 18 November). For the logarithmic results for this year, the period spanned 67 days from 30 September through 6 December. Some improvement was noticeable to the end of the simulation (day 357) for the 1979 data set, but this improvement was limited to about 0.3° C.

Model-Suggested Target Temperature Modifications

108. Since the model-proposed target modifications found in Tables 2 and 3 differed for the two years, a means of combining the two sets of proposed targets was needed. Several alternatives presented themselves. First, the use of the union of the two modification sets was examined. These sets included several modifications that were uniquely beneficial for one year or the other, but not both. The common set of modifications, therefore, contained several undesirable modifications. A much more conservative approach would have been to adopt only those modifications that were proposed by both years. This resulted in a common set of suggested modifications that had very few elements.

109. As previously mentioned, modifications during the spring and summer were often not suggested because operations could not be influenced by any amount of target temperature increase. The ports selected by the daily operations were already as high in the pool as was possible. Modification of the targets in the positive direction would, therefore, neither increase nor decrease the objective function value as no change in the release temperature would be effected. Therefore, if modifications were suggested for one year but not for the other, they could be adopted for both years and ignored for the year that they effected no physical change. This method produced a common set of modifications that was more liberal than an intersection of the two

sets proposed by the individual years and more conservative than the union of the same two sets.

110. This process was followed for both the linear and the logarithmic objective function results. The resulting modifications are shown in Table 4. When these modifications were applied to the targets from Table 1, the revised target scenarios in Table 5 resulted. The proposed modified target temperatures and the original target temperatures are plotted for the linear and the logarithmic objective function work in Figure 25.

111. The overall agreement between the release targets and the releases using daily operations was good with an daily average absolute error of 1.3° C for the 1978 data set and 1.1° C for the 1979 data set. However, the timing of the errors was of extreme importance. The spring and summer targets for both years were met closely; but in the fall, which has been identified as exceptionally critical for the fishery, the errors were large, often exceeding 4° C. Therefore, if spring and summer deviations from the prescribed targets of the magnitudes shown in Table 4 are acceptable, some modifications to the original target temperatures may be beneficial.

112. The amount of modification suggested depends upon the relative importance of meeting the release target temperatures during the different priority periods. If the relationship between the different period weightings is linear (i.e., a 1-, 2-, 3-type weighting), the revised target set under the linear objective in Table 5 should be adopted. However, if improvement during the high-priority periods warrants more substantial sacrifices during the lower priority periods, perhaps the logarithmic objective function (with a 1-, 10-, 100-type relationship among the priorities) is more appropriate. In this case, the revised target temperature set under the logarithmic objective should be chosen.

Table 4

Common Modification Sets

Date	Suggested Modifications: Linear Objective °C	Suggested Modifications: Logarithmic Objective °C
Jan 01-31	0.0	0.0
Feb 01-28	0.0	0.0
Mar 01-18	0.0	0.0
Mar 19-25	+2.5	+2.5
Mar 26-01	+2.5	↓
Apr 02-08	+2.5	↓
Apr 09-15	+1.4	↓
Apr 16-22	+2.0	↓
Apr 23-29	+1.4	↓
Apr 30-06	+1.4	↓
May 07-13	+2.5	↓
May 14-20	0	↓
May 21-27	+2.5	↓
May 28-03	+2.5	↓
Jun 04-10	+2.5	↓
Jun 11-17	+1.4	↓
Jun 18-24	0	↓
Jun 25-01	+1.4	↓
Jul 02-08	+1.4	↓
Jul 09-15	+1.4	↓
Jul 16-22	+1.4	↓
Jul 23-29	0	↓
Jul 30-05	+1.4	↓
Aug 06-12	+2.5	+1.4
Aug 13-19	0	+2.5
Aug 20-25	↓	0
Aug 27-02	↓	↓
Sep 03-09	↓	↓
Sep 10-16	↓	↓
Sep 17-23	↓	↓
Sep 24-30	+1.4	↓
Oct 01-07	0	↓
Oct 08-14	+2.0	↓
Oct 15-31	0	↓
Nov 01-30	0	↓
Dec 01-31	0	↓

Table 5

Original and Modified Target Temperature Scenarios

Date	Original Target Temperature, °C	Modified With Linear Objective, °C	Modified With Logarithmic Objective, °C
Jan 01-31	3.0	3.0	3.0
Feb 01-28	3.0	3.0	3.0
Mar 01-06	4.7	4.7	4.7
Mar 07-13	4.9	4.9	4.9
Mar 14-18	5.3	5.3	5.3
Mar 19-20	5.3	7.8	7.8
Mar 21-31	5.5	8.0	8.0
Apr 01-06	5.8	8.3	8.3
Apr 07-08	6.3	8.8	8.8
Apr 09-14	6.3	7.7	8.8
Apr 15	6.9	8.3	9.4
Apr 16-20	6.9	8.9	9.4
Apr 21-22	7.6	9.6	10.1
Apr 23-30	7.6	9.6	10.1
May 01-06	8.2	9.6	10.7
May 07-13	8.5	11.0	11.0
May 14-20	8.5	8.5	11.0
May 21-31	9.0	11.5	11.5
Jun 01-10	↓	9.0	↓
Jun 11-17		11.5	
Jun 18-24		9.0	
Jun 25-30		10.4	
Jul 01-13		10.4	
Jul 14-22	11.1	12.5	13.6
Jul 23-29	11.1	11.1	13.6
Jul 30-31	11.1	12.5	13.6
Aug 01-05	12.8	14.2	15.3
Aug 06-12	12.8	14.2	15.3
Aug 13-19	12.8	12.8	12.8
Aug 20-31	12.8	12.8	12.8
Sep 01-06	11.6	11.6	11.6
Sep 07-13	10.9	10.9	10.9
Sep 14-20	6.7	6.7	6.7
Sep 21-23	6.0	6.0	6.0
Sep 24-30	6.0	7.4	6.0
Oct 01-07	5.2	5.2	5.2
Oct 08-13	4.5	6.5	4.5
Oct 14	4.0	6.0	4.0
Oct 15-20	4.0	4.0	4.0
Oct 21-31	3.0	3.0	3.0
Nov 01-30	3.0	3.0	3.0
Dec 01-31	3.0	3.0	3.0

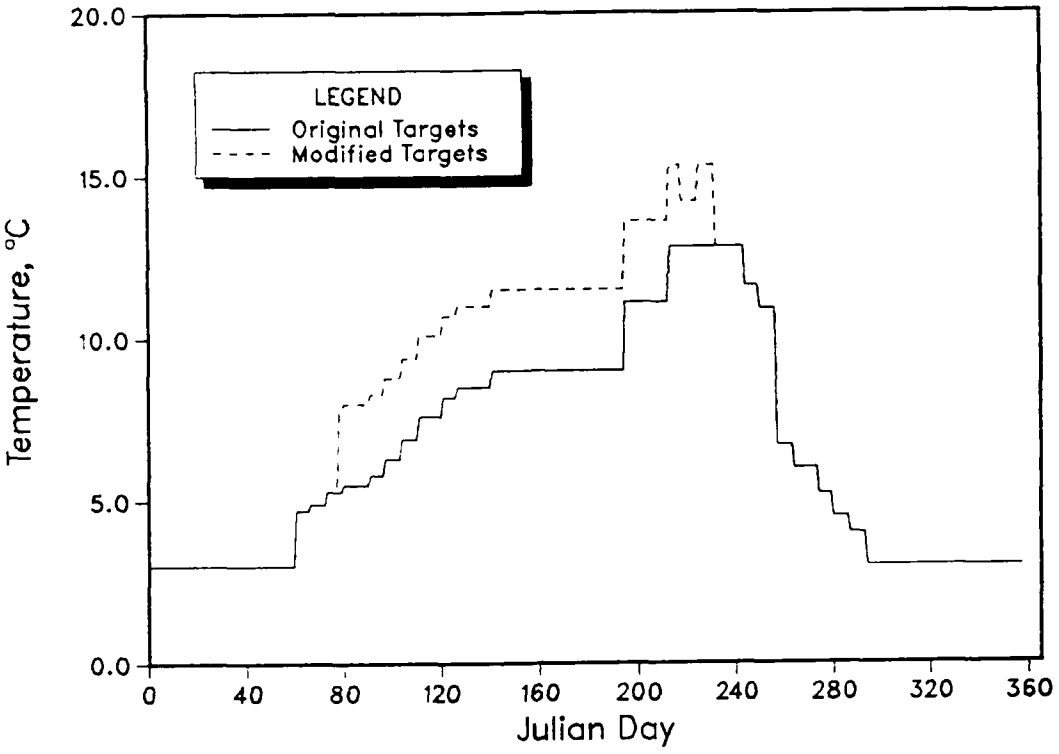

a. Linear

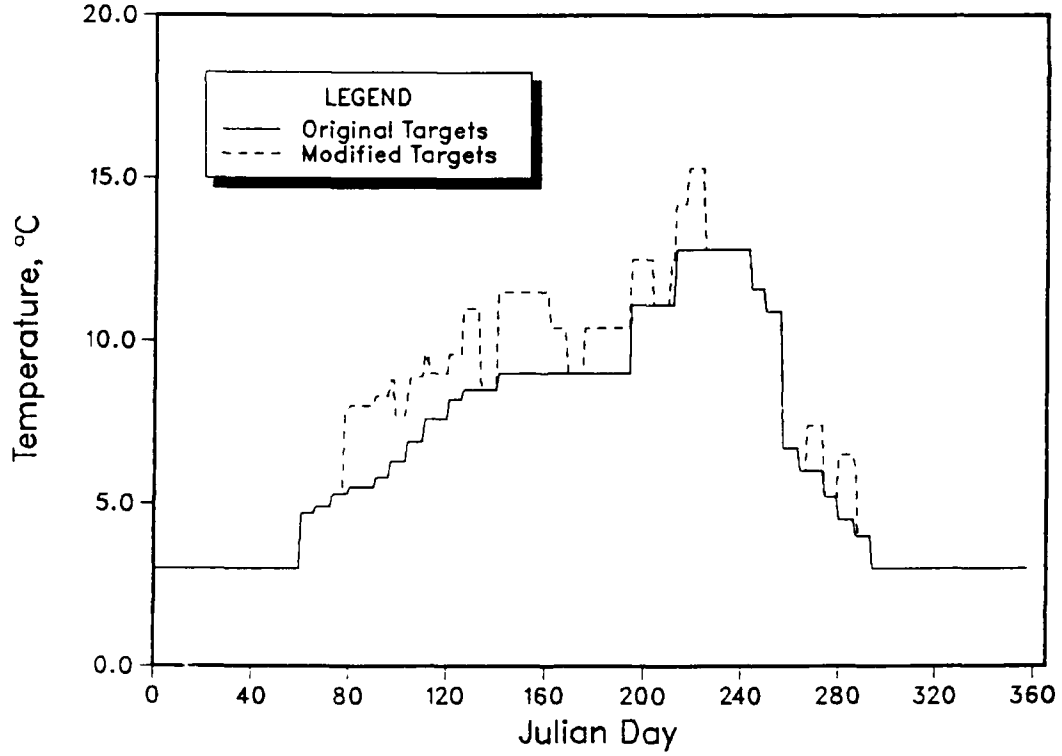

b. Logarithmic

Figure 25. Original and revised target temperature sets for the linear and logarithmic objective optimizations

PART V: RESULTS AND CONCLUSIONS

113. An in-depth investigation of the operational characteristics of the Lost Creek Lake intake structure was performed. This investigation was undertaken to evaluate the potential for improving the reservoir release water temperatures to better suit the downstream fishery. The investigation was a combined physical and numerical modeling effort designed to produce a selective withdrawal description, a simultaneous multilevel single-wet-well operation description, and an estimation of the capacity for long-term operational improvements.

114. The selective withdrawal results from the model testing were very encouraging when compared to previous model studies. The effective angles of withdrawal for the port levels compared favorably to research results. The lateral constriction of the near-field topography impacted the withdrawal zone limits in a logical manner. The previously developed empirical descriptions for withdrawal profile shape and maximum velocity location applied well to the model data. These facts tended to substantiate the credibility of the selective withdrawal model predictions for this structure.

115. The development of a site-specific, simultaneous, multilevel, single-wet-well withdrawal (more commonly, blending) description also followed previous work. The hydraulic descriptions for the port levels were first determined through physical model testing. The existing version of a separately developed blending algorithm was then applied to the model results under stratified pool conditions. Only minor changes to the blending algorithm were necessary. The comparison between the predicted and observed data was excellent. From this work and the selective withdrawal work, a new version of the SELECT model was produced for the daily operation of the Lost Creek Dam intake structure that will be provided to Portland District.

116. An evaluation of the potential for improving the seasonal operation of the Lost Creek intake structure for release temperature maintenance was also performed. The results of this study indicated that some potential exists for improvement of the high-priority fall release water temperatures at the expense of the lower priority summer releases. However, large sacrifices, often requiring that the current release target be missed by as much as 4.5° C for short periods and 3° C for longer periods during the spring and summer, were necessary to produce an improvement in the fall, which was generally less

than 2.5° C. The maximum period during which a significant (greater than 0.5° C) continuous improvement was realized was 67 days for the adopted criteria. This was far short of the length of the substantial deviations between release temperatures and targets, but may be worthwhile, nonetheless. Regardless of the operational strategy adopted during the summer and fall, the meteorology drives the pool toward a common thermal condition. By Julian day 345 (early December), the optimized and nonoptimized pool conditions were essentially indistinguishable for 1978 and were very close for 1979. Release temperatures after this were within 0.5° C of best-daily operations, regardless of the optimization.

117. The results of this operational evaluation were somewhat subjective in nature stemming from the all-important objective function equation. The question concerning the relationship among the individual priorities, whether linear or logarithmic, was important in determining the number and size of the target temperature modifications proposed. The results using the logarithmic relationship, based on a heavy weighting on the priority system, advised large modifications of the target scenario for most of the period with less than top priority. The linear objective function equation advised fewer and smaller modifications, but produced a measurable impact on fall releases. The optimization work produced three clear choices. The benefits and costs must be weighed by the concerned parties to determine whether to use the set of targets produced by the logarithmic objective function, those produced by the linear objective function, or the targets now in place.

118. An important consideration in the application of the results of this study is the limitation of existing data. The modifications suggested were based upon only 2 years of simulations. Confident extrapolation of the results from these simulations to years with vastly different hydrologic and/or meteorologic conditions may not be possible. However, these can easily be evaluated with the verified model.

119. The products of these evaluations were an accurate description of the selective withdrawal characteristics of this structure, a description of the blending processes, and a clear choice concerning long-term operational strategies. The coupled use of the selective withdrawal description and the blending description provides a means of predicting the best possible port combination for a given stratification pattern and release quantity to achieve a release target. The choice remaining concerning operational strategies is

simply one of relative worth. If achieving cooler fall releases regardless of significantly warmer than desired summer releases is the objective, the modified target scenario identified earlier by the use of the logarithmic objective function should be adopted. If some spring and summer deviations can be tolerated, but not as large as those from the logarithmic objective function work, the targets from the linear objective function work should be used. If the sacrifices from these alternatives are considered too large, the best best-daily operations can be obtained using the port selection and selective withdrawal information derived from this study. Use of this information should provide release temperatures very near the current targets between days 60 and 260, with a loss of coolwater resources in the fall.

REFERENCES

Bohan, J. P., and Grace, J. L., Jr. 1973 (Mar). "Selective Withdrawal from Man-Made Lakes," Technical Report H-73-4, US Army Engineer Waterways Experiment Station, Vicksburg, Miss.

Cassidy, R. A., and Johnson, E. B. 1982 (Mar). "Chronology of a Public Participation Decision to Fill a Pacific Northwest Reservoir," Canadian Water Resources Journal, Vol 7, No. 2, pp 90-111.

Cassidy, R. A., Larson, D. W., and Putney, M. R. 1981. "Physicochemical Limnology of a New Reservoir," Proceedings, Symposium on Surface-Water Impoundments, Hydraulics Division, American Society of Civil Engineers H. S. Stefan, ed., pp 1465-1473.

Cramer, S. P., Satterthwaite, T. D., Boyce, R. R., and McPherson, B. P. 1985. "Impacts of Lost Creek Dam on the Biology of Anadromous Salmonids in the Rogue River," Phase I Completion Report, Oregon Department of Fish and Wildlife, Portland, Oreg.

Davis, J. E., Holland, J. P., Schneider, M. L., and Wilhelms, S. C. 1987 (Mar). "SELECT: A Numerical, One-Dimensional Model for Selective Withdrawal," Instruction Report E-87-2, US Army Waterways Experiment Station, Vicksburg, Miss.

Fontaine, D. G., Labadie, J. W., and Loftis, B. 1982 (Feb). "Optimal Control of Reservoir Discharge Quality Through Selective Withdrawal," Technical Report E-82-1, prepared by Colorado State University and the US Army Engineer Waterways Experiment Station, Vicksburg, Miss.

Holland, J. P. 1982 (Apr). "Effects of Storage Reallocation on Thermal Characteristics of Cowanesque Lake, Pennsylvania," Technical Report HL-82-9, US Army Engineer Waterways Experiment Station, Vicksburg, Miss.

Howington, S. E. 1988 (Feb). "Multi-Ported, Single Wet Well Intake Structure operation in a Stratified Reservoir," Presented at the Symposium on Water Quality, Charleston, S. C., available from Hydrologic Engineering Center, Davis, Calif.

_____. "Simultaneous, Multiple-Level Withdrawal from a Density Stratified Reservoir" (in preparation), US Army Engineer Waterways Experiment Station, Vicksburg, Miss.

Leggett, R. W., and Williams, L. R. 1981. "A Reliability Index for Models," Ecological Modeling, Vol 13, pp 303-312.

Martin, J. L. 1986 (Mar). "Application of a Two-Dimesnional Model of Hydrodynamics and Water Quality (CE-QUAL-W2) to DeGray Lake, Arkansas," Technical Report E-87-1, US Army Engineer Waterways Experiment Station, Vicksburg, Miss.

Miller, D. S. 1978. Internal Flow Systems, Vol 5, BHRA Fluid Engineering Series, British Hydromechanics Research Association.

Smith, D. R., Wilhelms, S. C., Holland, J. P., Dortch, M. S., and Davis, J. E. 1987 (Mar). "Improved Description of Selective Withdrawal Through Point Sinks," Technical Report E-87-2, US Army Engineer Waterways Experiment Station, Vicksburg, Miss.

US Army Corps of Engineers, "Hydraulic Design Criteria," prepared for Office, Chief of Engineers, by the US Army Engineer Waterways Experiment Station, Vicksburg, Miss., issued serially since 1952.

US Army Engineer District, Portland. 1966. "Lost Creek Dam, Hydrology and Meteorology," Design Memorandum No. 2, Portland, Oreg.

_____. 1979 (Jun). "Lost Creek Lake Annual Water Quality Report, 1978," Portland, Oreg.

_____. 1980 (Sep). "Lost Creek Lake Annual Water Quality Report, 1979," Portland, Oreg.

_____. 1983. "Rogue River Basin Project," Portland, Oreg.

Wilhelms, S. C., and Schneider, M. L. 1986 (May). "Operational Tools: Optimal Control of Reservoir Water Quality," Proceedings, CE Workshop on Design and Operation of Selective Withdrawal Intake Structures, San Francisco, Calif; also available as Miscellaneous Paper HL-86-3, US Army Engineer Waterways Experiment Station, Vicksburg, Miss.

Wlosinski, J. H. 1984. "Evaluation of Techniques for CE-QUAL-R1: A One-Dimensional Reservoir Water Quality Model," Miscellaneous Paper E-84-1, US Army Engineer Waterways Experiment Station, Vicksburg, Miss.

APPENDIX A: WITHDRAWAL ANGLE TEST RESULTS

Table A1

Withdrawal Angle Test Results

Test No.	Level	Upper Limit El	Upper Limit θ Deg	Lower Limit El	Lower Limit θ Deg
2	2	--	--	1,734.5	137
3	2	--	--	1,726.4	157
4	2	--	--	1,728.3	166
5	2	--	--	1,734.4	126
8	3	--	--	1,688.3	109
11	4	1,705.3	78	--	--
12	4	1,699.9	81	1,598.8	60
15	5	1,641.4	98	--	--
16	4	1,717.0	68	--	--
17	2	--	--	1,749.3	124
23	2	--	--	1,748.9	132
24	4	1,706.0	87	1,588.9	64
25	3	1,802.7	64	1,675.3	115
27	4	1,710.0	72	1,588.3	57
101	3	--	--	1,679.6	71
102	4	1,720.3	60	1,594.9	47
103	4	1,703.8	95	1,587.1	68
104	4	1,724.5	46	--	--
105	2	--	--	1,758.9	133
106	4	1,695.3	78	1,590.7	41
107	4	1,696.5	76	1,590.0	39
108	3	1,794.5	25	1,668.5	81
109	↓	1,803.7	73	1,678.5	108
110	↓	1,803.6	64	1,678.4	85
111	↓	1,810.0	67	1,675.9	102
112	↓	1,802.7	67	1,687.1	81
113	↓	1,816.7	67	1,673.3	96
114	5	1,679.2	89	--	--
115	5	1,677.0	48	--	--
117	5	1,693.5	101	--	--
118	1	--	--	1,778.2	146
119	1	--	--	1,770.1	195
120	1	--	--	1,796.4	191
122	5	1,668.9	94	--	--

Note: Dashes indicate boundary interference.

APPENDIX B: COMPUTATION OF THE RELIABILITY INDEX

1. The Reliability Index (RI) was proposed by Leggett and Williams (1981)* as a general test that can be used to evaluate the correspondence, or goodness of fit, between predicted values from mathematical models and observed data. Thus, the test allows inference of a model's predictive capability. An interpretation of the index is that it indicates, in some sense, the degree to which predictions and observations agree. An RI of 1.0 indicates a perfect agreement, and the RI increases as predicted and observed values diverge. The RI is computed from

$$RI = \frac{1 + \sqrt{\frac{1}{N} \sum_{t=1}^{T} \sum_{n=1}^{N} \frac{1 - (Y_{tn}/X_{tn})}{1 + (Y_{tn}/X_{tn})}^2}}{1 - \sqrt{\frac{1}{N} \sum_{t=1}^{T} \sum_{n=1}^{N} \left[\frac{1 - (Y_{tn}/X_{tn})}{1 + (Y_{tn}/X_{tn})}\right]^2}} \qquad \text{(B1)}$$

where

N = number of x,y pairs for a specific sampling period

T = number of sampling periods

t = index for sampling periods

n = index for x,y pairs

Y = observed value

X = model-predicted value

2. Some caution must be exercised when interpreting the RI since it is affected by variability in observations as well as the degree of correspondence between observed and predicted values. It is a measure of a model's capabilities only to the degree to which the observed data are considered "true." However, comparisons between simulations with a given model, or between different models, which result in a smaller RI for the same observed data would generally indicate an improvement. The RI was compared to other commonly used statistical tests by Wlosinski (1984) and was considered the best statistic for aggregating model results.

---

* This discussion was taken from Martin (1986). All references cited in this Appendix are listed in the References at the end of the main text.